

CHARACTERIZATION OF ORGANOSULFUR COMPOUNDS
WITH ELECTROSPRAY IONIZATION/MASS SPECTROMETRY

THESIS

Presented to the Graduate Council of
Southwest Texas State University
in Partial Fulfillment of the Requirements

For the Degree of
Master of Science

By

Yi Zhang

San Marcos, Texas
August, 2002

ACKNOWLEDGEMENTS

I would like to give my deepest and most sincere appreciation to Dr. Walter Rudzinski, my advisor, professor in the Chemistry and Biochemistry Department, for his consistent guidance, trust, support and patience throughout this research. It is truly a great experience to work with him, a person who is always considerate, willing to help and absolutely helpful.

My sincere thanks go to my committee members, Dr. Linette Watkins and Dr. Ross Compton, for their valuable suggestions and helpful discussions.

A special thank is extended to Mr. Dan Millikin for his help with the instruments and his little gifts which always make me feel warm. Special thanks to all the faculty staff and graduate students in the Chemistry and Biochemistry Department of SWT, for their friendship and assistance.

Finally, I would like to express my profound gratitude and respect for my dearest families, for their encouragement and love throughout my life.

TABLE OF CONTENTS

LIST OF TABLES	vi
LIST OF FIGURES	vii
ABSTRACT	viii
Chapter	
I. INTRODUCTION	1
Mass Spectrometry	1
Electrospray Ionization (ESI)	3
The Quadrupole Ion Trap	5
Tandem Mass Spectrometry in the Ion Trap	6
Separation and Isolation of Organosulfur Compounds in Crude Oil	8
Mass Spectrometry of Organosulfur Compounds	10
II. EXPERIMENT	13
Reagents and Chemicals	13
Preparation of Standard Solution	13
PdCl ₂ Stock Solution	13
Organosulfur Standard Solution	14
Organosulfur Standard Mixture	14
Organosulfur Standard Mixture in Tufflo	15
Sample Solution for Organosulfur: PdCl ₂ Ratio Study	15
Fractionation Procedure for the Maya Crude Oil Distillate	16
Instrumentation	17
Injection System	18
ESI Ionization Source	18
Ion Optics	20
Quadrupole Ion Trap	20
Collision Energy for MS/MS Experiments	21
III. RESULTS AND DISCUSSION	22
ESI/MS Spectrum of PdCl ₂ in (50:50) Methanol: Acetonitrile	22
ESI/MS Full Mass Scan of Organosulfur Standard Compounds	27
ESI/MS Full Mass Scan of an Organosulfur Standards Mixture	29
Optimization of Source Fragmentation Energy (Cone Voltage)	30

Concentration Effects.....	33
Effect of Concentration Ratio between Organosulfur Compounds and PdCl ₂	35
ESI/MS of Standard Compounds Mixture in Tufflo.....	37
ESI/MS/MS of Organo Sulfur Compounds	38
Full Scan Mode.....	38
MS/MS SIM Mode	42
Effect of Collision Energy	44
ESI/MS and MS/MS of Maya Crude Oil Fractions	47
 IV. CONCLUSION.....	 51
 REFERENCES	 52

LIST OF TABLES

Table 3.1 Abundance of Pd and Cl Isotopes.....	24
Table 3.2 Formulae and Isotopes of Pd Complexes	25
Table 3.3 Absolute and Relative Intensity of Each Organosulfur Standard in the Mixture	30
Table 3.4 Study of Ratio between DBT and PdCl ₂	36

LIST OF FIGURES

Figure 2.1	Structures of Standard Organosulfur Compounds.....	14
Figure 2.2	Scheme for the LEC Fractionation of Maya Crude Oil.....	16
Figure 3.1	MS Full Scan of 22.5 mM PdCl ₂	23
Figure 3.2	Effect of Capillary Temperature on the Formation of Pd Complexes	26
Figure 3.3	MS Full Scan of DBT, BNTP and Thianthrene	28
Figure 3.4	Charge Transfer Reaction between Pd Complex and DBT.....	28
Figure 3.5	MS Full scan of Standard Mixture	29
Figure 3.6	Effect of Source Fragmentation Energy on Molecular Ions Signals of DBT and Pd Complexes	31
Figure 3.7	Effect of Source Fragmentation Energy on BNTP and Thianthrene	33
Figure 3.8	Variation of Molecular Ion Signal Intensity with Concentration for Several Organosulfur Standards	34
Figure 3.9	MS Full Scan of Standards Mixture in Tufflo.....	37
Figure 3.10	MS/MS Full Scan Data for Standards Mixture	38
Figure 3.11	ESI/MS ³ Full Scan of Thianthrene	39
Figure 3.12	The Mechanism of Hydrogen Loss	40
Figure 3.13	Cleavage Reactions of Radical Cation	40
Figure 3.14	Fragmentation Mechanism of DBT.....	41
Figure 3.15	Fragmentation Mechanism of 2-DBT	42
Figure 3.16	MS/MS SIM Data for Standards Mixture of DBT, Thianthrene, BNTP, 2-DBT and 4,6-DBT.....	43
Figure 3.17	Effect of Ion Trap Collision Energy on Fragmentation of DBT and BNTP	45
Figure 3.18	Effect of Ion Trap Collision Energy on Fragmentation of 2-DBT and 4,6-DBT	46
Figure 3.19	MS Full Scan of Maya Crude Oil Fractions.....	47
Figure 3.20	MS/MS Full Scan Data for Maya Crude Oil.....	48
Figure 3.21	The Possible Structure of the Compound with M.W. 237 in CMPASH	50

ABSTRACT

CHARACTERIZATION OF ORGANOSULFUR COMPOUNDS WITH ELECTROSPRAY IONIZATION/ MASS SPECTROMETRY

By

Yi Zhang, B.S.

Southwest Texas State University

August 2002

SUPERVISING PROFESSOR: Dr. Walter Rudzinski

The goal of this research was to use tandem mass spectrometry (MS/MS) in an ion trap to analyze for organosulfur compounds in crude oil. Five organosulfur standard compounds were analyzed by electrospray ionization/mass spectrometry (ESI/MS) and MS/MS using PdCl₂ as a sensitivity enhancing reagent. Radical cations were formed by a charge transfer reaction between palladium and the sulfur compounds in the gas phase. For tandem mass spectrometry experiments, a 32 Dalton neutral loss (S) was observed for dibenzothiophene (DBT), thianthrene and benzonaphthothiophene (BNTP); and a 33 Dalton loss (HS) was observed for 2-methyl-dibenzothiophene (2-DBT) and 4,6-dimethyl-dibenzothiophene (4,6-DBT). ESI/MS and MS/MS scans were performed in

both full scan and single ion monitoring (SIM) mode. Effects of some variables on the formation of molecular ions or molecular fragmentation were studied to optimize the method, including sample concentration, cone voltage, collision energy and concentration ratio between PdCl₂ and sulfur compounds. A standard mixture of organosulfur compounds was put in a hydrogenated white oil (Tufflo) to mimic the chemical environment of the crude oil. MS and MS/MS experiments were performed. A Maya crude oil distillate of 200-350°C was fractionated using the saturate-aromatics-resins-asphaltenes (SARA) method followed by ligand exchange chromatography in order to concentrate organosulfur components. ESI/MS and MS/MS experiments were performed on the fractions.

CHAPTER I

INTRODUCTION

1.1 Mass Spectrometry

Mass spectrometry (MS) is an analytical method for separating and identifying chemical species based on mass-to-charge (m/z) ratio. A mass spectrum is a record of the relative abundance of these species as a function of m/z . MS has an outstanding position among analytical methods due to its high sensitivity, low detection limits and diversity of applications. MS has progressed extremely rapidly during the last decade in production, separation and detection of ions, data acquisition and data reduction [1].

The major working principal of MS is described as following. First, a molecular ion in the gas phase is produced in an ionization source, and this molecular ion may also fragment to form other product ions in the ionization source. Second, all these ions formed from the original compound are delivered into a mass analyzer to be separated according to m/z ratio and detected in proportion to their abundance. Finally a mass spectrum of the molecule is thus produced, which can be presented as a graph or as a table. A mass spectrum provides information about molecular weight, chemical structure and functional groups.

A mass spectrometer always consists of the following elements: a device to introduce the compound that is analyzed, e.g. a liquid chromatograph or a direct

insertion probe; an ionization source to produce ions from the sample; one or several analyzers to separate the various ions based on m/z ratio; a detector to count the ions emerging from the last analyzer and to measure their abundance; a computer to process the data, produce the spectrum and control the instrument through feedback. Among these components, the ionization source and mass analyzer have received the most attention.

A variety of ionization techniques are used for MS, such as electron ionization (EI), chemical ionization (CI), fast atom/ion bombardment (FAB) and secondary ion mass spectrometry (SIMS), thermospray (TSP), electrospray (ESI) and atmospheric pressure chemical ionization (APCI). These ionization techniques use different working strategies, possess different characteristics and therefore are suitable for different chemical species. The most important considerations are the internal energy transferred during the ionization process and the physicochemical properties of the analyte. ESI is a soft ionization technique, which transfers ions from solution to the gas phase. Since its introduction in 1984, ESI/MS has become a method of outstanding importance and has a variety of applications [2]. ESI was used in this research as the ionization source.

Just as there are a great variety of ion sources, there are many different analyzers, including quadrupole analyzer, quadrupole ion trap, time-of-flight (TOF) analyzer, magnetic and electromagnetic analyzers, etc. They are differentiated by their working mechanisms and instrumentation. The quadrupole ion trap was the analyzer used for this research.

Combining several analyzers in sequence for tandem mass spectrometry (MS/MS) is becoming common in order to obtain more detailed structural information about

compounds. An ion trap instrument, which is capable of multiple stage MS (MS^n , $n>2$) in the time domain, was used for MS/MS in this research.

1.2 Electrospray Ionization (ESI)

Electrospray ionization is an example of an atmospheric pressure ionization (API) process. This technique transfers ions from solution to the gas phase by ionizing the sample at atmospheric pressure and then transferring the ions into a mass spectrometer. The success of ESI began when Fenn et al [3] showed that multiply charged ions could be obtained from proteins, allowing their molecular weight to be determined with instruments whose mass range only extended to as low as 2000 Da. In the beginning, ESI was considered to be an ionization source only dedicated to protein analysis. Later on, its use was extended not only to other polymers and biopolymers but also to the analysis of small polar molecules. It appears, indeed, that ESI allows for the analysis of a wide range of molecules and it is easy to couple to high-performance liquid chromatography (HPLC), micro-HPLC or capillary electrophoresis. Electrospray principles and biological applications were reviewed extensively in 1996 [4], 1997 [2] and 2000 [5].

An electrospray [1-2] is produced by applying a strong electric field, under atmospheric pressure, to a liquid passing through a capillary tube with a weak flux (normally 1-10 $\mu\text{l}/\text{min}$). The electric field is obtained by applying a potential difference of 3-6 kV between this capillary and the counter-electrode, separated by 0.3-2 cm,

producing an electric field on the order of 10^6 V/m. This field induces a charge accumulation at the liquid surface located at the end of the capillary, and thus charged droplets are produced. This is the first major step in the production of gas-phase ions by electrospray from electrolyte ions in solution. When the charged droplets shrink into ultimately very small highly charged droplets by solvent evaporation, the electrical charge density at the surface of the droplets increases. The small droplets produce gas-phase ions by either an ion evaporation mechanism or charged residue mechanism [2]. The ion evaporation mechanism predicts that after the radii of the droplets decrease to a given size, direct ion emission from the droplets becomes possible. While the charged residue mechanism predicts that eventually a small droplet will have a single analyte molecule, which accommodates charge at the sites offering the most stable gas-phase stability. A curtain of heated inert gas, most often nitrogen, or a heated capillary helps to remove the remaining solvent molecules.

ESI is a soft ionization technique because fragmentation of ions can be avoided. Generally ESI requires a more polar solvent, e.g., water, methanol or acetonitrile, and sometimes the addition of an acid or base in order to promote ionization.

ESI has important characteristics: first, it is able to produce multiply charged ions from large molecules. Second, the formation of ions is a result of the electrochemical process and of the accumulation of charge in the droplets. Generally, ions are formed either through protonation of basic groups or deprotonation of acidic groups depending on the characteristics of the solvent. Third, the electrospray current is limited by the electrochemical process that occurs at the probe tip and it is sensitive to concentration

rather than to the total amount of sample, except at very low flow rates on the order of $\mu\text{L}/\text{min}$.

In ESI, a large number of variables influence the ionization process, including the nature of the solvent, flow, nature and size of the capillary, distance to the counter-electrode, etc. Furthermore, the efficiency of the ionization process depends on surface tension, nature of the analytes and electrolytes, presence of other analytes and electrochemical processes at the probe tip [1].

The ESI source has been coupled to a number of different mass analyzers including: quadrupole, triple quadrupole, ion trap, double focusing magnetic sector, time-of-flight and FT-ICR.

1.3 The Quadrupole Ion Trap [1]

The quadrupole is a device that uses the stability of ion trajectories in oscillating electric fields to separate ions according to their m/z ratio. The quadrupole ion store or ion trap is based on the same principle.

Quadrupole ion analyzers are made up of four perfectly parallel rods with circular or, ideally, hyperbolic sections. The quadrupole ion trap is made up of a circular electrode, with two ellipsoid caps on the top and the bottom. An ion trap can be imagined as a quadrupole bent on itself in order to form a closed loop. The inner rod is reduced to a point at the center of the trap, the outer rod is the circular electrode and the top and bottom rods make up the caps.

The overlapping of a direct potential with an alternating one gives a kind of three-dimensional quadrupole in which the ions of all masses are trapped on a three-

dimensional trajectory. A resonant frequency along the z-axis is applied to expel the ions of a given mass.

In quadrupole instruments, the potentials are adjusted so that only ions with a selected mass go through the rods. The principle is different in an ion trap. Ions with different masses are present together inside the trap and are expelled according to their masses so as to obtain the spectrum. As the ions repel each other in the trap, their trajectories expand as a function of time. To avoid ion losses by this expansion, the trajectory needs to be reduced. Therefore, a pressure of helium gas is maintained in the trap to remove excess energy from the ions by collision.

Ions produced in the ionization source are focused through a skimmer and two RF-only octopoles. Differential pumping provides a vacuum in the trap while the source is at atmospheric pressure. A gating lens limits the number of injected ions to an acceptable limit. After ion injection, ions of different masses are stored together in the trap and then analyzed according to their mass. Most commercial traps operate by applying a fundamental RF voltage on the ring. Its frequency is constant, but its amplitude voltage can be varied. Additional RF voltage of selected frequency and amplitudes can be applied to the end caps. Mass analysis in the ion trap can be by ion ejection at the stability limit or by resonant ejection. The Finnigan ion trap mass analyzer, which was used in this research performs mass analysis via resonant ejection.

1.4 Tandem Mass Spectrometry in the Ion Trap

Tandem mass spectrometry, abbreviated MS/MS, is a general method involving at least two stages of mass analysis, either in conjunction with a dissociation process or a

chemical reaction that causes a change in the mass or a charge of an ion [6-8]. MS/MS experiments provide structural information of samples by giving fragments of the original compound. Therefore, tandem MS is also a good tool to identify species with specific functional groups in a complicated molecule.

Basically, a tandem mass spectrometry experiment can be conceived in two ways [1]: in space by the coupling of two physically distinct analysis; or in time by performing an appropriate sequence of events in an ion storage device. In an ion trap, time dependent tandem MS occurs rather than space dependent tandem MS. The general sequence of operations is:

1. Select an ion of one m/z ratio by expelling all the others from the ion trap. This can be performed either by selecting the precursor ion at the apex of the stability diagram or by resonant expulsion of all ions except for the selected precursor.
2. Let the ions fragment. Energy is provided by collision with the helium gas. This fragmentation can be improved by excitation of the selected ions by irradiation at their secular frequency.
3. Analyze the ions by one of the two scanning methods: stability limit or resonant ejection.
4. Alternatively, select a fragment in the trap and let it fragment further. This step can be repeated to provide MS^n spectra.

In this research, MS/MS and MS^3 experiments were performed to characterize organosulfur compounds, organosulfur compounds in a hydrogenated hydrocarbon matrix and organosulfur compounds in a Maya crude oil.

1.5 Separation and Isolation of Organosulfur Compounds in Crude Oil

Crude oil is a naturally occurring, flammable liquid whose chemical composition varies depending upon the source. Crude oil and refinery products primarily consist of hydrocarbons (50-90%) with the remainder composed of compounds containing N, S, O, and trace amounts of organometallics. The sulfur content in coal and petroleum products generally ranges from 0.025 to 11%, and thus creates a potential pollution problem upon combustion due to the production of sulfur dioxide, a major component of acid rain [9]. With the increasing consumption of fossil fuel, legislators have mandated stricter controls on sulfur dioxide emissions. New legislation in Japan and Europe will limit the sulfur content in light oil to 50 parts per million (ppm) maximum by 2005. The United States will limit the sulfur content to 15 ppm by the middle of 2006. Inorganic sulfur can be successfully removed from crude oil by a variety of physical separation methods, but organosulfur compounds are much more difficult to eliminate. Even though a variety of techniques [10] have been used to isolate and remove the sulfur, further developments are necessary in order to meet regulatory requirements.

One of the main forms of organic sulfur in fossil fuels and many of their industrial conversion products are thiophenes. A large part of this sulfur is bound in polycyclic aromatic sulfur heterocycles (PASHs), which in oil mainly consist of alkylated benzothiophenes (BTs) and dibenzothiophenes (DBTs) [11].

Isolation and separation of organosulfur from crude oil is the first step in analysis. Since the properties of polyaromatic sulfur compounds are very similar to those of polyaromatic hydrocarbons, finding a suitable isolation procedure is a difficult task. The nucleophilic interaction of sulfur compounds with PdCl_2 to form complexes has been

well documented in the literature [12-16]. Nishioka et al successfully exploited this effect and developed a unique separation method based on the saturates-aromatics-resins-asphaltenes (SARA) approach followed by ligand exchange chromatography (LEC) using PdCl_2 and CuCl_2 on silica gel columns [12-13, 17-20]. CuCl_2 can be used to isolate aliphatic sulfur compounds like thiophenols and sulfides [19], while PdCl_2 can be used to separate PASH compounds [17]. Andersson disclosed some deficiencies in the Nishioka method; i.e., the elution of organosulfur compounds as PdCl_2 complexes, incomplete recovery of benzothiophenes, and the early elution of constituents with terminal thiophene rings [21]. Furthermore, the selectivity of the PdCl_2 varies with the organosulfur ring size. Rudzinski and coworkers [22] found that the selectivity decreased in the order 3-ring > 2-ring > 1-ring PASH compounds.

In order to analyze different fractions of a Maya crude oil, Rudzinski and coworkers isolated and characterized sulfur compounds in the aliphatic and aromatic fractions of a crude oil [22-25] separated using the Nishioka Method [17,19]. In their research, the SARA method was used to separate the crude oil into saturate, aromatic, resin and asphaltene fractions. CuCl_2 silica was then used to separate the aliphatics into sulfur containing aliphatics (CMA_{aliph-S}) and aliphatic fractions, while PdCl_2 silica was used to separate the aromatics into polyaromatic hydrocarbons (CMPAH), polyaromatic sulfur heterocycles (CMPASH), and sulfur-polar aromatic compounds (CMSPAC). Although the separation of sulfur containing compounds was not completely selective, the amount of sulfur in the CMA_{aliph-S} fraction was nine times as large as in the aliphatic CMA_{aliph} fraction, while the amount of sulfur in the CMPASH and CMSPAC fractions was 1.5 and 1.9 times as much as in the CMPAH fraction. The PdCl_2 silica is not nearly as selective

for aromatic sulfur compounds as the CuCl_2 is for the separation of aliphatic sulfur compounds. The fractions collected were analyzed by a combination of elemental analysis, Fourier transform infrared, ^1H and ^{13}C nuclear magnetic resonance (NMR), gel permeation chromatography (GPC), and atmospheric pressure chemical ionization/ mass spectrometry (APCI/MS) [25].

1.6 Mass Spectrometry of Organosulfur Compounds

Developing a selective mass spectrometry procedure for sulfur compounds is not easy, because the properties of polyaromatic sulfur compounds are very similar to those of polyaromatic hydrocarbons, which are present in crude oil in abundance. Therefore a combination of ionization conditions, e.g. electrospray, ion-molecule reactions and/or derivatization may be desirable in order to direct fragmentation along a unique pathway, which can then be used to identify the organosulfur compounds.

Hunt and Shabanowitz [26] developed a rapid qualitative analysis of sulfur compounds which is selective in hydrocarbon matrices and which affords the relative abundance and molecular weight of the organosulfur compounds plus information about the structural environment of the sulfur atom in the molecules under analysis. The method combines chemical ionization and collision activated dissociation (CAD) on a Finnigan triple quadrupole mass spectrometer. Neutral loss resulting from a loss of HS were prominent in the spectra. By setting quadrupole number 1 and quadrupole 3 to scan repetitively at a fixed mass separation, the detector monitored organosulfur compounds exclusively.

A highly selective tandem mass spectrometer was used as a liquid chromatographic detector for the quantification of dibenzothiophene (DBT) in crude petroleum oil and in an alternate fuel oil [27]. The triple quadrupole mass spectrometer was used in the single-ion monitoring (SIM) mode, the first quadrupole being set for a m/z 184 (corresponding to M^+ for DBT) and the second for a m/z 152 (corresponding to $[M-32]^+$).

Another approach for the analysis of PASH compounds involves the oxidation of the sulfur to the sulfone with *m*-chloroperbenzoic acid. Rudzinski et al evaluated the oxidation approach for the analysis of DBT and found a sensitivity enhancement of 500 for the sulfone over the parent DBT [22].

Bayer et al developed coordination-ion-spray-MS (CIS-MS), a relatively new method of chemical ionization, in which positively or negatively charged complexes may be formed by the addition of a suitable coordinating atom to the analytes, which imparts charge so that complexes can be detected by mass spectrometry [28]. Generally elements from the first and eighth transition groups are employed, e.g., Cu^{+1} , Ni^{+2} , Pd^{+2} , Pt^{2+} and Ag^{+1} . These form highly stable π bonding complexes with both alkenes and polynuclear aromatic compounds. Since both polar and nonpolar organic compounds can form coordination compounds with an appropriate central atom, this form of ionization is highly versatile. Neither an electric field nor the formation of a reagent gas plasma by corona discharge is necessary for ionization. Efficient nebulization in the ion source is however required. Since pneumatic nebulization in the absence of an electric field is often insufficient to obtain a suitable spray, a supporting voltage usually must be applied in order to stabilize the nebulization process.

Recently, Rudzinski et al developed a method of coordination ion spray in which Pd^{2+} in methanol was added to the electrospray ionization (ESI) source of an ion trap mass spectrometer [22-23]. The addition of the Pd^{2+} produces charge transfer complexes with 3- and 4- ring organosulfur compounds, which can dissociate to form radical cations $[\text{M}]^+$.

CHAPTER II

EXPERIMENT

2.1 Reagent and Chemicals

Methanol, acetonitrile (CH_3CN), hexane, chloroform (CHCl_3), dichloromethane (CH_2Cl_2), toluene, and diethyl ether were obtained from EM Science (Gibbstown, NJ); Maya crude oil, from Mobil Corporation (Beaumont, TX); and Tufflo, from Exxon Mobil; Alumina (60/80 mesh) was obtained from The Coast Engineering Laboratory (Redondo Beach CA); PdCl_2 and silica gel (70-270 mesh) were obtained from Aldrich (Milwaukee, WI). The organosulfur compounds: thiophene, benzothiophene (BT), dibenzothiophene (DBT), thianthrene, benzonaphthothiophene (BNTP) 4,6-dimethyl-dibenzothiophene (4,6-DBT) were obtained from Aldrich and 2-methyl-dibenzothiophene (2-DBT) from Sigma-Aldrich (Milwaukee, WI). Fig. 2.1 shows the structure and formula weight (F.W.) of each of the standards.

2.2 Preparation of Standard Solutions

2.2.1 PdCl_2 Stock Solution

8.0 mg PdCl_2 was dissolved in 2 ml (50:50) methanol: acetonitrile. After 1-2 hours, the red PdCl_2 powder was totally dissolved and turned into a clear yellow solution with a concentration of 22 mM.

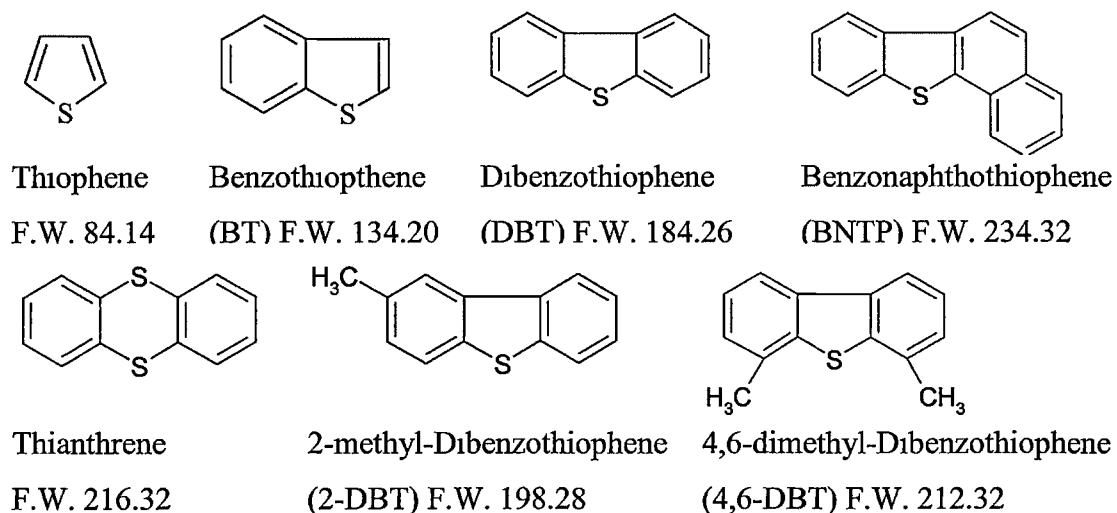


Fig. 2.1 Structures of standard organosulfur compounds.

2.2.2 Organosulfur Standard Solution

The following compounds were each mixed with 9.0 mg PdCl₂: 2.0 mg DBT, 2.3 mg BNTP, 2.2 mg thianthrene, 2.0 mg 2-DBT and 2.5 mg 4,6-DBT. Each mixture was dissolved in 10 ml (50:50) methanol: acetonitrile. The concentration of each solution was 1.1 mM DBT; 0.97 mM BNTP; 1.0 mM thianthrene; 1.0 mM 2-DBT and 1.2 mM 4,6-DBT. The concentration of PdCl₂ for every sample solution was 5 mM.

2.2.3 Organosulfur Standard Mixture

The following compounds were mixed together and dissolved in 10 ml (50:50) methanol: acetonitrile: 2.0 mg DBT, 2.1 mg BNTP, 2.3 mg thianthrene, 2.0 mg 2-DBT, 2.1 mg 4,6-DBT and 4.4 mg PdCl₂. The concentration of each component was 1.1mM DBT; 0.90 mM BNTP; 0.92 mM thianthrene; 1.0 mM 2-DBT; 1.0 mM 4,6-DBT and 2.5 mM PdCl₂. Assuming the reactivity of each sulfur compound with PdCl₂ is equal, for

each sulfur compound, the concentration ratio (Sulfur: PdCl₂) was 1: 0.5. The stock solution was later diluted to a series of solution to perform the concentration study.

2.2.4 Organosulfur Standards Mixture in Tufflo

Tufflo is a clear and viscous liquid, which has been extensively hydrogenated and consists of hydrocarbons, the major components in crude oil. In order to apply the characterization method developed with standard compounds to a real crude oil sample, it was believed necessary to put the standards in a chemical environment similar to the actual crude oil. Sulfur represents 2-3% abundance by weight of Maya crude oil. If we assume 250 is the average molecular weight of the sulfur containing compounds [25] 20% is the average weight abundance of sulfur-containing compounds in crude oil. To approximate this amount, 3.5 mg DBT, 4.2 mg BNTP, 4.2 mg thianthrene, 3.5 mg 2-DBT and 4.0 mg 4,6-DBT were added to 0.1 g Tufflo.

The sulfur compounds were dispersed uniformly in Tufflo by stirring the mixture with a spatula. 0.01g of this mixture was then dissolved in 1ml (50:50) methanol: acetonitrile containing 0.025 mmol PdCl₂. The molar ratio of each sulfur compound to PdCl₂ was at most 1:10. The mixture was only partly dissolved in the solvent.

2.2.5 Sample Solutions for Organosulfur: PdCl₂ Ratio Study

The DBT solution of 1mM was used to study the effects of the ratio between the organosulfur compounds and PdCl₂. 5mM PdCl₂ and 1mM, 0.5mM, 0.25mM, and 0.1mM DBT in (50:50) methanol: acetonitrile were used.

2.3 Fractionation Procedure for the Maya Crude Oil Distillate

Sulfur-containing aromatic compounds were isolated from Maya crude oil distillate, 200°C-350°C, by using the SARA method followed by ligand exchange chromatography (LEC). The fractionation scheme for the isolation of sulfur-containing compounds is illustrated in Fig. 2.2.

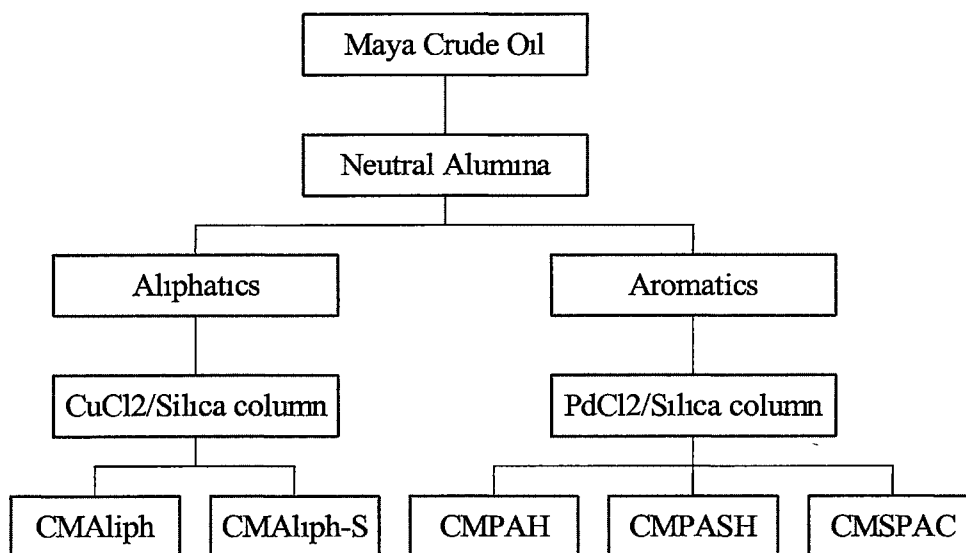


Fig.2.2 Scheme for the LEC fractionation of the aliphatic+ aromatic fractions of a Maya crude oil.

Alumina was dried at 200°C overnight. PdCl₂ /silica was prepared by mixing 20 g of silica gel with 1g of PdCl₂ suspended in an aqueous solution. The sorbent was dried in an oven at 95°C overnight, then held at 200°C for 24 hours prior to use.

Approximately 0.2g of Maya crude oil distillate was dissolved in 5mL CH₂Cl₂. This mixture was absorbed onto 3g of neutral alumina. The solvent was removed under a gentle stream of nitrogen gas. The alumina with the adsorbed sample was then packed on top of 6g neutral alumina in a 10×125 mm column. The sample was eluted first with

20mL hexane, which removes the aliphatics. The aromatics were then eluted with 50mL of toluene. Solvents were removed from the aliphatics and the aromatics by rotary evaporation.

The aromatics were then dissolved in 5mL CH_2Cl_2 and absorbed onto 0.5g of the PdCl_2 / silica gel. The solvent was evaporated under a gentle stream of nitrogen gas, and the mixture was packed on top of 5.0g PdCl_2 / silica gel in a 10×125 mm column. 30 mL CHCl_3 : hexane (1:1) was used to elute the CMPAH fraction. A further 50mL of the same eluent was used to elute the CMPASH fraction. 100 mL of CHCl_3 : diethyl ether (9:1) was used to elute the CMSPAC fraction.

After the fractionation procedure described above, CMPASH with PdCl_2 was obtained in CHCl_3 : hexane (1:1) and CMSPAC with PdCl_2 was obtained in CHCl_3 : diethyl ether (9:1). The solvents were removed by rotary evaporation. 10mg of residue from the two fractions were dissolved in 1mL (50:50) methanol: acetonitrile respectively for ESI/MS and MS^2 experiments.

The separation of the aliphatics into CMA_{aliph} and CMA_{aliph-S} has been previously described [22-24].

2.4 Instrumentation

Mass spectra were obtained on a Finnigan LCQ ion trap MS equipped with atmospheric pressure chemical ionization (APCI) or electrospray ionization (ESI) sources. A Gateway 2000 computer with Navigator 2.1 software was used for collection and analysis of the data. ESI positive (ESI+) was used in this research. MS and MS^2 were

performed in full scan mode as well as in single ion monitoring (SIM) mode. Each scan was the average of 3 microscans and data for the MS spectra were based on 10 scans.

2.4.1 Injection System

The LCQ includes an electronically controlled, integrated, dual syringe pump. The syringe pump delivers sample solution from the syringe to the ESI source via a pusher block. The pusher block is driven by a motor to depress the plunger of the syringe at a controlled rate.

For premixed solutions used in this research, a 250 μ L Unimetrics syringe was used. The flow injection rate was 3 μ L/min.

For experiments involving tee mixing before the ESI source, two 250 μ L Hamilton syringes in parallel were used. The flow rate for both syringes was 1.5 μ L/min.

2.4.2 ESI Ionization Source

Instrumental parameters for the ESI ionization source were consistently applied to every sample in this research, including sheath gas flow rate, auxiliary gas flow rate, ion spray voltage, capillary temperature, capillary voltage, tube lens offset and source fragmentation energy.

Sheath gas flow rate was 60 (arbitrary units). The sheath gas is the inner coaxial nitrogen gas that sprays (nebulizes) the sample solution into a fine mist as it exits the sample tube. Typical sheath gas flow rates for ESI are 60 units for sample flow rates of 3 μ L/min. The auxiliary gas flow rate was 0. The auxiliary gas is the outer coaxial nitrogen gas that assists the sheath gas in the nebulization and evaporation of sample solutions. The auxiliary gas also helps lower the humidity in the ion source. Typical

auxiliary gas flow rates for ESI are 10-20 units. However, auxiliary gas is usually not needed for sample flow rates below 100 $\mu\text{L}/\text{min}$.

The ion spray voltage was 3.5kV. This large positive or negative (ESI-) voltage is applied to the ESI needle, which sprays the sample solution into a fine mist of charged droplets. Typically the value of the spray voltage is ± 4.5 kV to ± 5 kV. Considering PdCl_2 was added to help form cation complexes of sulfur compounds, the ion spray voltage was decreased to 3.5kV.

The capillary temperature was 200°C. The heated capillary assists in desolvating ions that are produced by the ESI. The heated capillary is behind the aperture in the center of the spray shield. Ions are drawn into the heated capillary in the atmospheric pressure region and transported to the capillary-skimmer region of the vacuum manifold by a decreasing pressure gradient. The capillary voltage was 10 V. This potential assists in propelling ions from the heated capillary to the skimmer.

Ions from the heated capillary enter the tube lens. The tube lens has a mass dependent potential applied to it to focus the ions toward the opening of the skimmer. The tube lens offset voltage is an additional potential of between 0- ± 40 V applied to the tube lens to accelerate the ions into the background gas (helium) that is present in the capillary-skimmer region. Collision with the background gas aids in the desolvation of the ions and increases sensitivity. If the tube lens offset voltage is too high, collision with the background gas can be energetic enough to cause ions to fragment. This fragmentation, called ion source CID, decreases sensitivity. When tuning the instrument, the tube lens offset voltage was optimized to maximize sensitivity by balancing desolvation with fragmentation. Generally, the tube lens offset was about 30V.

Source fragmentation energy (cone voltage), was applied to introduce in-source fragmentation. The value of the voltage was optimized to obtain a good S/N ratio for each sample and is reported with each Figure in Chapter 3.

2.4.3 Ion Optics

The ion optics of the mass spectrometer transmit ions from the ESI source to the mass analyzer. The ion optics consist of two octapoles and an interoctapole lens. Each octapole is an octagonal array of cylindrical rods that acts as an ion transmission device. A RF voltage and dc offset voltage (-10 to +10 V) that are applied to the rods give rise to an electric field that guides the ions along the axis of the octapole. During ion transmission, the offset voltage is negative for positive ions and positive for negative ions. The two octapoles are separated by the interoctapole lens, which assists in the focusing and gating of ions. For each sample, the potentials that are applied to the octapoles and interoctapole lens were optimized to maximize the ion current to the mass analyzer.

2.4.5 Quadrupole Ion Trap

The quadrupole ion trap is the site of mass analysis, which includes ion isolation, CID and ion ejection. The primary relevant parameters are ring electrode RF voltage, ion injection waveform voltage, ion isolation waveform voltage and resonance excitation RF voltage. They are automatically optimized by the instrument.

The ring electrode RF voltage produces a three-dimensional quadrupole field within the mass analyzer cavity. This time-varying field drives ionic motion in both the axial and radial direction.

The ion injection waveform voltage acts during the ion injection step to eject unwanted ions from the mass analyzer and allow the concentration of target ions. The ion isolation waveform voltage ejects all ions except those of a selected mass-to-charge ratio or narrow range of mass-to-charge ratios in combination with the ring electrode RF voltage. The difference between the ion injection waveform voltage and the ion isolation waveform voltage is that the first one can be used for all scan modes, while the second one acts during the ion isolation step of single ion monitoring (SIM), single reaction monitoring (SRM) and MSⁿ (n>1) full scan mode applications

The resonance excitation RF voltage is applied to the endcap electrodes to fragment parent ions into product ions. This RF voltage is not strong enough to eject an ion from the mass analyzer. However, ion motion in the axial direction is enhanced and the ion gains kinetic energy. After many collisions, the ion gains enough internal energy to cause it to dissociate into product ions. The product ions are then mass analyzed.

During ion scan out, the resonance ejection RF voltage facilitates the ejection of ions from the mass analyzer and thus improves mass resolution.

2.5 Collision Energy for MS/MS Experiments

Collision energy is the voltage introduced in ion trap, which provides kinetic energy to parent ions in order to facilitate their dissociation via colliding with inert gas molecules. The ion trap acts as a collision cell in this research. The values of collision energies used are reported with each spectrum of each sample in Chapter 3.

CHAPTER III

RESULTS AND DISCUSSION

3.1 ESI/MS Spectrum of PdCl₂ in (50:50) Methanol: Acetonitrile

PdCl₂ is a red, hygroscopic solid, soluble in water to give PdCl₂·2H₂O. Differential thermal analysis and x-ray diffraction studies indicate that there are at least three polymorphs, which depend on mode of preparation. Best known is α-PdCl₂, which is orthorhombic with two formula units in the unit cell. Its structure consists of infinite chains in which each Pd is surrounded by four coplanar bridging Cl atoms [29].

The MS full scan spectrum of PdCl₂ is shown as Fig.3.1(a) under the running conditions specified in section 2.4.2.

The +2 oxidation state is the most common state for Pd, and it easily forms complexes with many organic and inorganic species [29]. The mass spectral distributions at specific m/z ratios are due to the isotopes of Pd and Cl (Table 3.1).

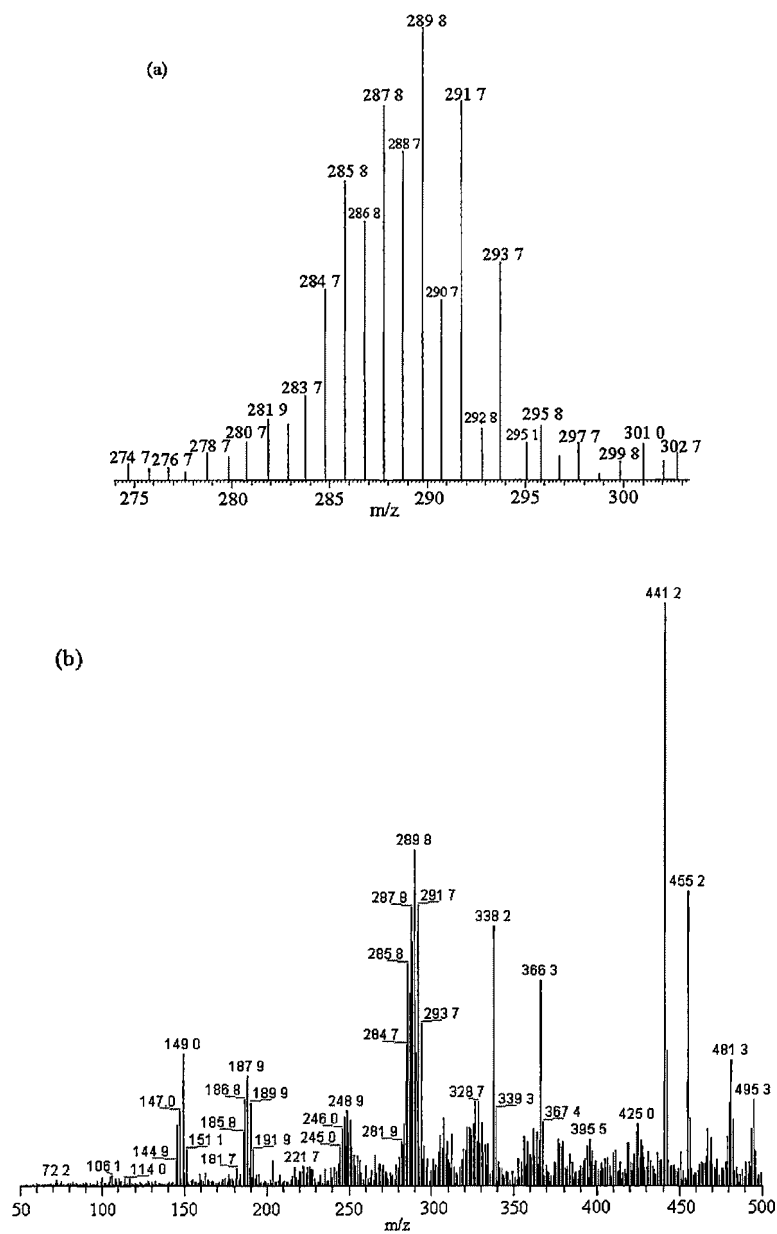


Fig.3.1 MS full scan of 22.5mM PdCl₂ in (50:50) CH₃OH: CH₃CN.

Mass range: (a) 274-303 D, (b) 50-500 D. Ion spray voltage, 3.5kV and source fragmentation energy, 0V.

Isotopes(Pd)	Abundance (%)	Isotope(Cl)	Abundance (%)
Pd ¹⁰²	1	Cl ³⁵	75.5
Pd ¹⁰⁴	11	Cl ³⁷	24.5
Pd ¹⁰⁵	22		
Pd ¹⁰⁶	27		
Pd ¹⁰⁸	27		
Pd ¹¹⁰	12		

Table 3.1: Abundance of Pd and Cl isotopes.

In this study, Pd²⁺ exhibited complexes with methanol and acetonitrile in the gas phase. As demonstrated in Fig. 3.1(b), the spacing between the isotope peaks of the Pd complex was always 1. In other words, the difference in m/z was always an integer. Since the mass difference between Pd isotopes are either 2 or 1, it can be concluded that the complexes have a +1 charge. By assigning a molecular formula and then calculating the isotopic distribution around 149, 188, 249 and 290, the formulae for four of the Pd complexes were determined. They are [Pd(CH₃CN)]⁺, [Pd(CH₃CN)₂]⁺, [PdCl₂(CH₃CN)(CH₃OH)]⁺ and [Pd₂Cl(CH₃CN)]⁺ respectively. Depending upon the abundance of Pd and Cl isotopes, each peak of the four mass distributions was assigned a formula for the Pd complex. The isotopic distribution was calculated using Isopro 3.0 and the results are shown in Table 3.2. Isopro 3.0 is a program that affords information about the mass distributions of species with more than one isotope in MS spectra. The hypothetical mass distribution of [Pd₂Cl(CH₃CN)]⁺ exactly matches the distribution obtained. Except for [PdCl₂(MeCN)(MeOH)]⁺, the relative signal intensities of most peaks in each mass distribution correspond fairly well to the isotope abundance of Pd and Cl and the deviations are below ± 20%.

$[\text{Pd}(\text{MeCN})]^+$				$[\text{Pd}(\text{MeCN})_2]^+$			
m/z	Isotope	Cal. Abun. (%)	Act. Abun. (%)	m/z	Isotope	Cal. Abun. (%)	Act. Abun. (%)
145	Pd^{104}	11	8	186	Pd^{104}	11	14
146	Pd^{105}	22	18	187	Pd^{105}	22	24
147	Pd^{106}	27	23	188	Pd^{106}	27	30
149	Pd^{108}	27	40	190	Pd^{108}	27	22
151	Pd^{110}	12	11	192	Pd^{110}	12	10
$[\text{PdCl}_2(\text{MeCN})(\text{MeOH})]^+$				$[\text{Pd}_2\text{Cl}(\text{MeCN})]^+$			
m/z	Isotope	Cal. Abun. (%)	Act. Abun. (%)	m/z	Isotope	Cal. Abun. (%)	Act. Abun. (%)
245	$\text{Pd}^{102}\text{Cl}_2^{35}$	2	9	285	$\text{Pd}^{104}\text{Pd}^{105}\text{Cl}^{35}$	5	7
247	$\text{Pd}^{104}\text{Cl}_2^{35}$	13	17	286	$\text{Pd}_2^{105}\text{Cl}^{35}$	11	11
248	$\text{Pd}^{105}\text{Cl}_2^{35}$	26	10	287	$\text{Pd}^{105}\text{Pd}^{106}\text{Cl}^{35}$	13	10
249	$\text{Pd}^{106}\text{Cl}_2^{35}$	32	18	288	$\text{Pd}_2^{106}\text{Cl}^{35}$	16	14
250	$\text{Pd}^{105}\text{Cl}^{35}\text{Cl}^{37}$	8	13	289	$\text{Pd}^{105}\text{Pd}^{108}\text{Cl}^{35}$	13	12
251	$\text{Pd}^{104}\text{Cl}_2^{37}$	2	16	290	$\text{Pd}^{106}\text{Pd}^{108}\text{Cl}^{35}$	16	17
252	$\text{Pd}^{105}\text{Cl}_2^{37}$	3	9	291	$\text{Pd}_2^{106}\text{Cl}^{37}$	5	7
253	$\text{Pd}^{110}\text{Cl}_2^{35}$	14	8	292	$\text{Pd}_2^{108}\text{Cl}^{35}$	16	14
				294	$\text{Pd}_2^{108}\text{Cl}^{37}$	5	8

Table 3.2 Formulae and isotopes of Pd complexes in (50:50) methanol: acetonitrile. “Cal. Abun.” means “Calculated Abundance” and “Act. Abun.” means “actual Abundance”.

Changing the capillary temperature caused changes in the complexes observed. The spectra in Fig. 3.2 suggest that more Pd complexes with lower molecular weight form with an increase in capillary temperature in the range of 125-200 °C. This is because the heated

capillary helps to evaporate solvent. Therefore, increasing capillary temperature causes fewer solvent molecules to bond to Pd [2].

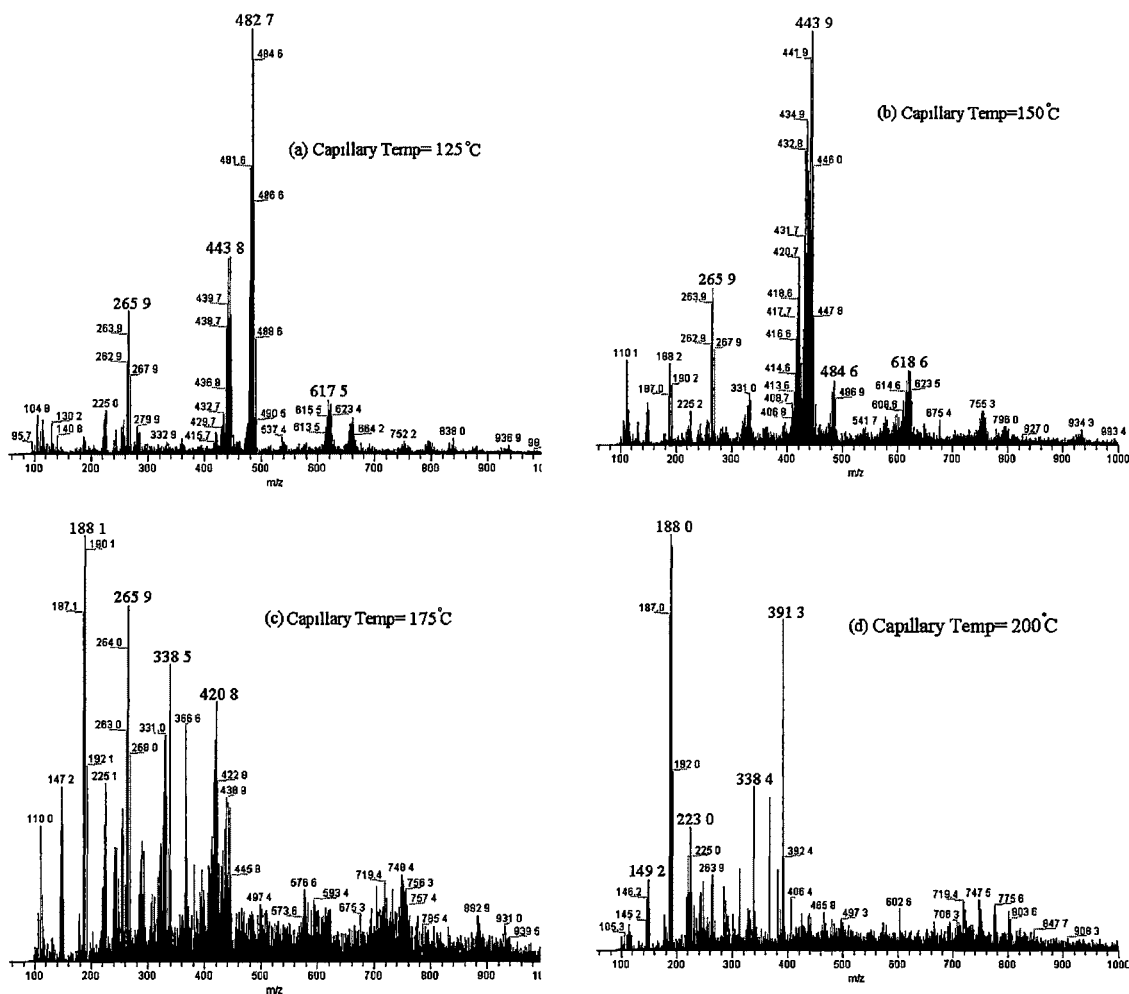


Fig. 3.2 Effect of capillary temperature on the formation of Pd complexes. Capillary temperatures are: (a) 125°C, (b) 150°C, (c) 175°C, and (d) 200°C. 5mM PdCl₂, in (50:50) methanol: acetonitrile, spray voltage, 3.5kV and source fragmentation energy, 0V.

For example, the complex with a mass distribution around m/z 483 evident in spectrum 3.2 (a) can be assigned a formula, [Pd¹⁰⁵Pd¹⁰⁶(CH₃CN)₅(CH₃OH)₂], while the complex at m/z 444 evident in spectrum 3.2 (b) is [Pd¹⁰⁵Pd¹⁰⁸(CH₃CN)₄(CH₃OH)₂]. On raising the temperature from 125°C to 150°C one acetonitrile molecule is evaporated.

The MS spectra of PdCl₂ are considered a blank control for the experiments described later in this chapter. Pd will be used to induce radical cation formation in organosulfur species. The relevant information obtained from the PdCl₂ control will help to distinguish signals due to Pd complexes from signals obtained from organosulfur compounds.

3.2 ESI/MS Full Mass Scan of Organosulfur Standard Compounds

Fig. 3.3 shows the MS full scan of DBT, BNTP and thianthrene with PdCl₂ in (50:50) methanol: acetonitrile. Each compound showed an intense molecular ion peak, with the signal intensity at or above 10⁶ at a concentration of 1mM with 5mM PdCl₂ in excess. In contrast, the Pd complexes discussed in section 3.1 had a relatively weaker response when compared with the sulfur compounds at a source fragmentation energy of about 10-25V. Thiophene and BT didn't show a response to the mass spectrometer and the same phenomenon has been described previously [22-23]. The ion source of the MS produces ions primarily by ionizing a neutral molecule through electron ejection, electron capture, protonation, deprotonation, adduct formation and the transfer of a charged species from the condensed phase to the gas phase [1]. Ion production often implies gas-phase ion-molecule reactions. For ESI, proton transfer reactions are a common ionization mechanism in the gas phase for most species. However, according to the MS results acquired for the three organosulfur compounds, molecular ions with +1 charge were formed without any mass change. Therefore, radical cations are forming in the presence of Pd⁺¹. Hence, the possible formation mechanism of radical cations of organosulfur compounds is probably due to charge transfer from the sulfur compounds to Pd⁺². The process is described for Pd and DBT in Fig. 3.4.

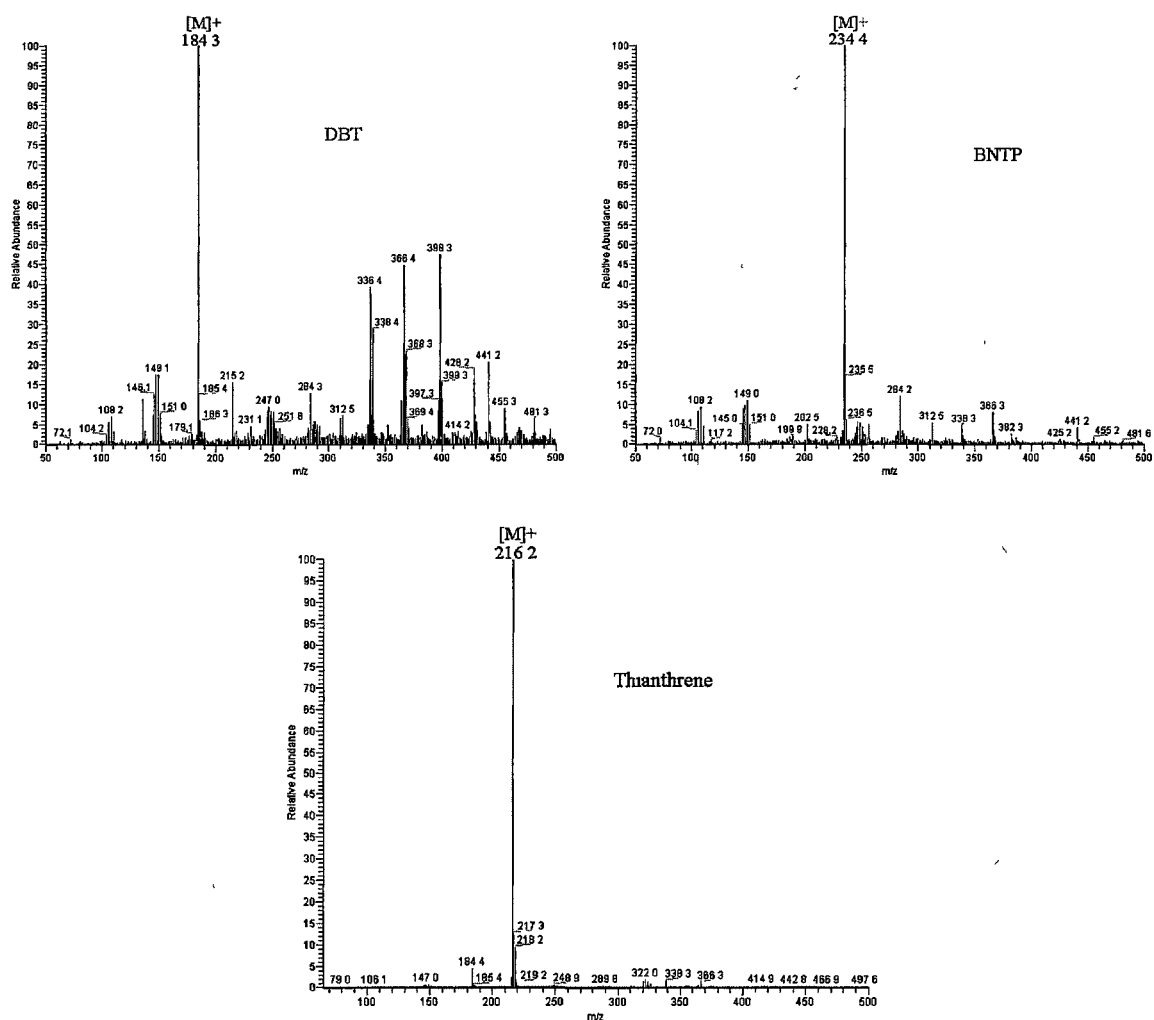


Fig. 3.3 MS full scan of DBT, BNTP and thianthrene. 1mM organosulfur compound with 5mM PdCl₂ in (50:50) methanol: acetonitrile. Spray voltage, 3.5kV; Capillary temperature, 200°C; Source fragmentation energy, 15V, 25V and 10V respectively.

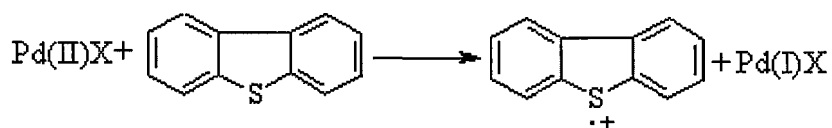


Fig 3.4. Charge transfer reaction between Pd complex and DBT.

3.3 ESI/MS Full Mass Scan of an Organosulfur Standards Mixture

In order to evaluate the relative response, the MS full scan of a mixture of five organosulfur compounds at equimolar concentration was performed. The MS full scan spectrum is shown as Fig. 3.5, while the absolute and relative signal intensity is shown in Table 3.3.

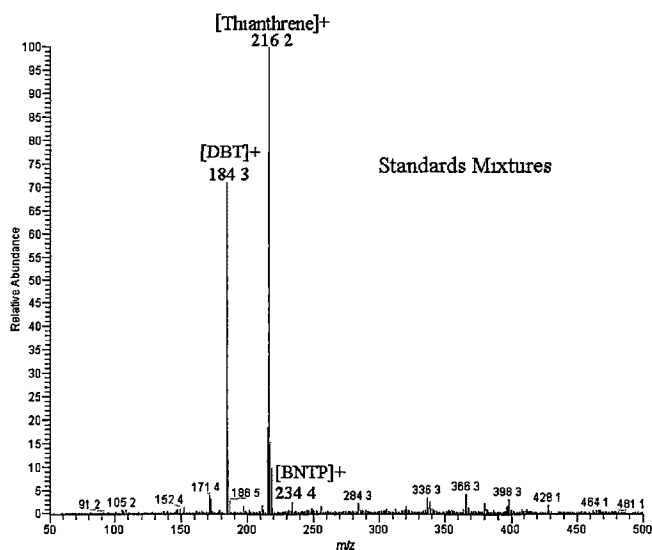


Fig. 3.5 MS full scan of standard mixture. 1mM DBT, BNTP, thianthrene, 2-DBT and 4,6-DBT in 2mM PdCl₂ in (50:50) methanol: acetonitrile; source fragmentation energy, 25V.

Thianthrene has the strongest signal intensity, which is probably due to its low ionization energy (7.7 eV) compared to DBT (7.9 eV) and BT (8.1 eV) [33]. The benzene ring in BNTP and the two methyl groups in 4,6-DBT next to the sulfur atom in their structures are thought to cause steric hindrance to Pd complexation, which precedes the charge transfer process. For this reason, BNTP and 4,6-DBT have relatively weak responses compared with DBT and thianthrene. 2-DBT doesn't have a strong response, even though the methyl group on position 2 doesn't provide steric hindrance to the complexation process. We do not have an explanation for this result. However, the reaction of losing a

hydrogen from a methyl group of the ion in the ion source may be partly responsible for the low signal intensity of the molecular ion of 2-DBT, which can also be one of the reasons causing low signal intensity for 4,6-DBT. The mechanism of fragmentation will be discussed in more detail in section 3.8.1. All of the five compounds have signals above 10^5 , which are above the signal/noise ratio.

	Molecular ion [M] ⁺	Intensity (10^5)	Relative Intensity (%)
DBT	184.3	198.6	71.1
2-DBT	197.3	4.4	1.6
4,6-DBT	211.3	4.6	1.7
Thianthrene	216.2	279.5	100.0
BNTP	234.4	6.7	2.4

Table 3.3 Absolute and relative intensity of each organosulfur standard in the mixture.

3.4 Optimization of Source Fragmentation Energy (Cone Voltage)

An increase in the source fragmentation energy causes in-source CID in the interface region between the ESI ionization source and the quadrupole ion trap mass analyzer. Considering signals from non-sulfur compounds as noise, in-source CID is important to enhance the signal to noise (S/N) ratio in MS full scan. The spectra in Fig. 3.6 qualitatively show the effect of in-source CID on DBT and palladium complexes.

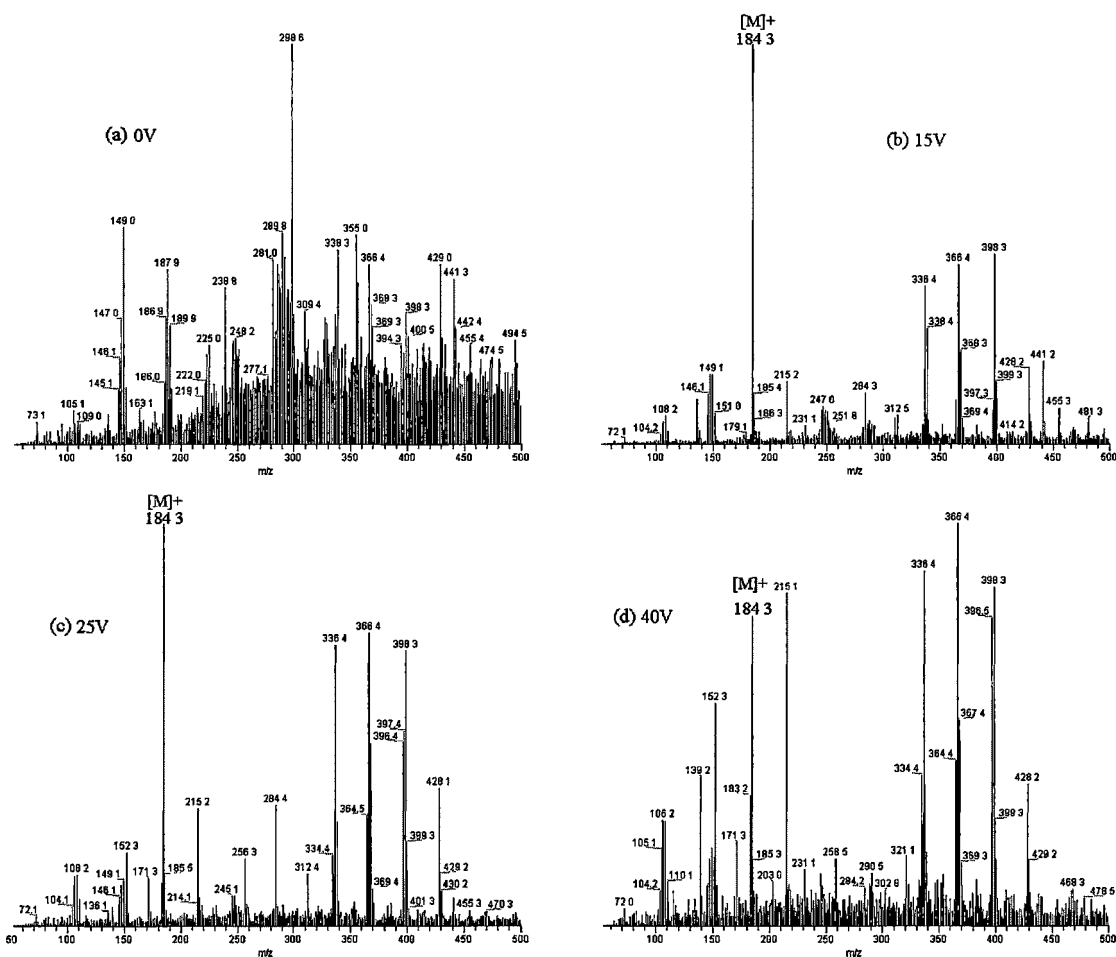


Fig. 3.6 Effect of source fragmentation energy on molecular ions signals of DBT and palladium complexes. (a) 0V, (b) 15V, (c) 25V and (d) 40V.

Without any source fragmentation energy, the DBT signal could not be distinguished from a noisy background, because signals due to palladium complexes have higher intensity. However, with the introduction of in-source fragmentation, DBT showed a strong and stable molecular ion peak in MS full scan mode and the S/N ratio was enhanced significantly. The possible reason for this phenomenon is that in-source fragmentation helps to break the palladium complexes and reduces the background signal.

If the source fragmentation energy continues to go up beyond an optimal value, the absolute signal intensity and the S/N ratio of the DBT molecular ion peak starts to decrease. The $[M-32]^+$ peak appears in the spectrum and the intensity of the $[M-32]$ peak increases with increasing source fragmentation energy. The results suggest that DBT starts to fragment by in-source CID even before entering the ion trap. A number of studies [1] have shown that as the electric field in the interface region between the ESI and the ion trap is increased, the kinetic energy transformed into internal energy also increases. The increasing internal energy causes the fragmentation of molecular ions. Therefore in-source CID causes a compromising result between the destruction of palladium complexes and fragmentation of the sulfur compounds. Every compound thus has an optimal source fragmentation energy.

In order to predict the effect of source fragmentation energy on sulfur compound decomposition, a quantitative study was initiated in which the source fragmentation energy applied to the samples were varied. Fig. 3.7 demonstrates the results for BNTP and thianthrene. The curves quantify the trend observed in the spectra. 5V and 10V source fragmentation energy are optimal for BNTP and thianthrene, respectively.

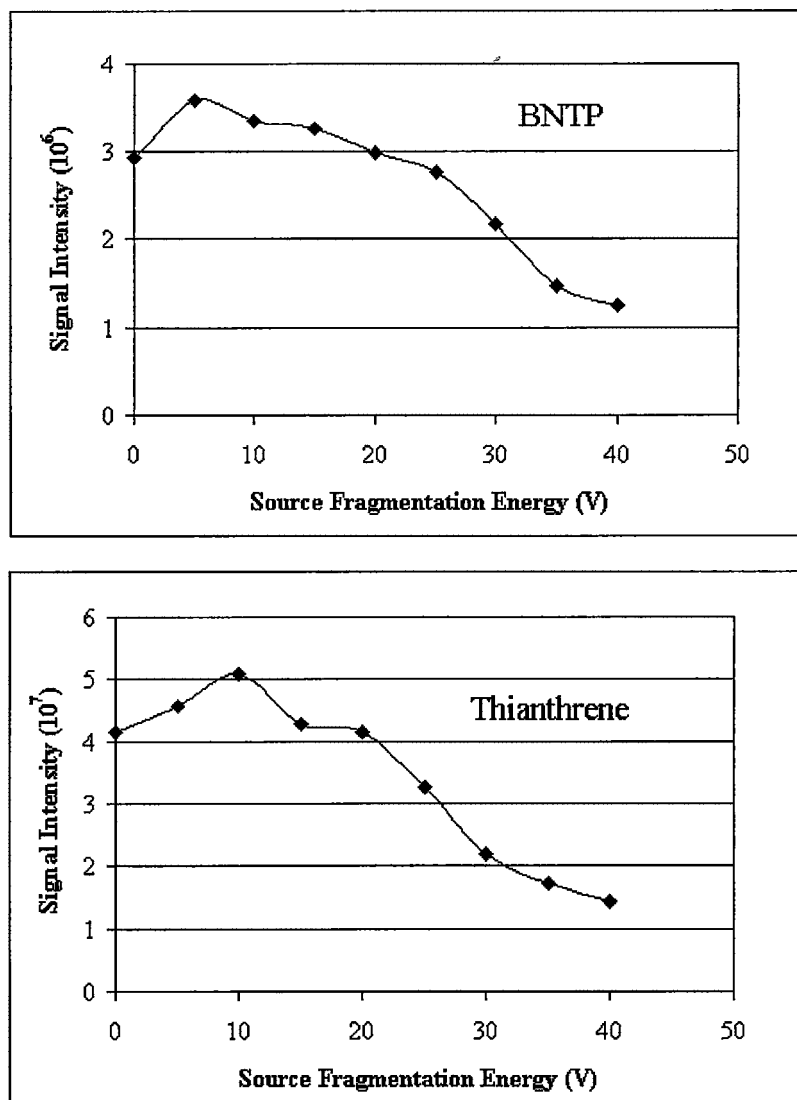


Fig. 3.7 Effect of Source Fragmentation Energy on BNTP and thianthrene. MS, full scan, 1mM standards and 5mM PdCl₂, in (50:50) CH₃OH: CH₃CN.

3.5 Concentration Effects

The effect of concentration on the molecular ion signal intensity of DBT, thianthrene, BNTP, 2-DBT and 4,6-DBT in a mixture is illustrated in Fig. 3.8 in full scan and SIM mode.

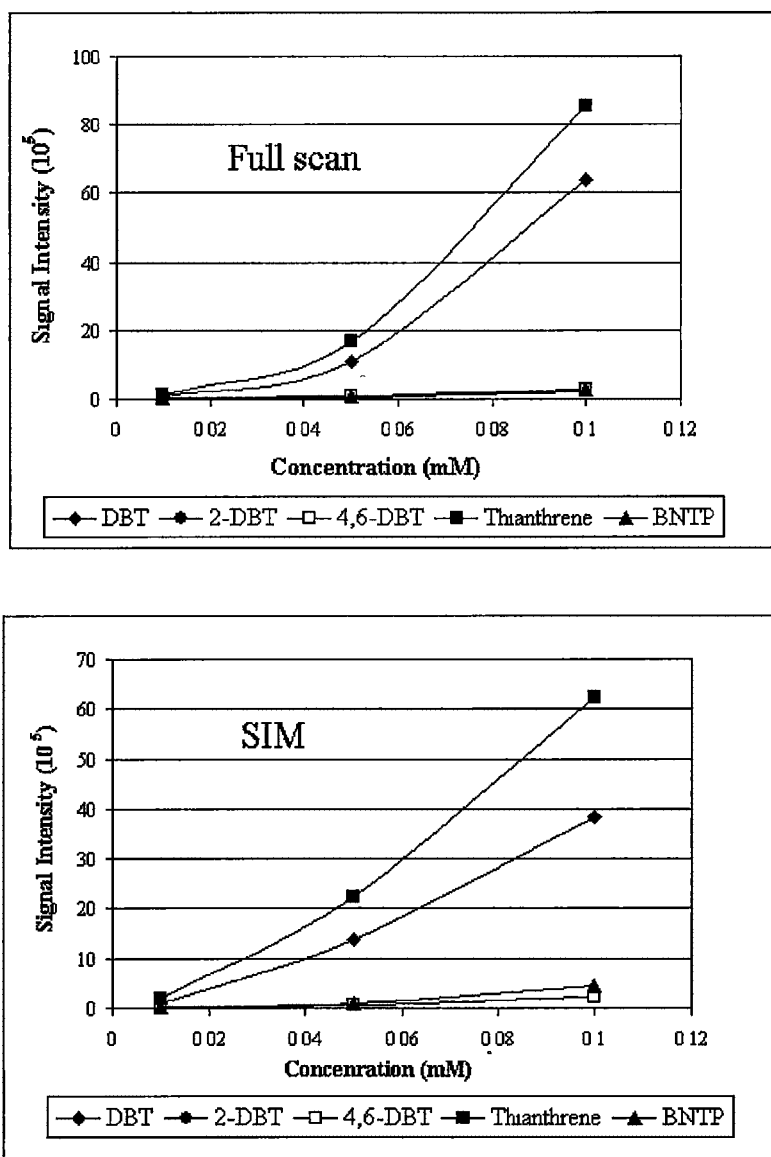


Fig. 3.8 Variation of molecular ion signal intensity with concentration for several organosulfur standards, Full scan and SIM mode in (50:50) CH₃OH: CH₃CN. Ratio of each sulfur standard to PdCl₂ is 1: 0.5.

One of the important features of ESI is its sensitivity to concentration, and not to the total quantity of sample injected in the source [2]. However, the typical relation between ESI-MS response and concentration is characterized by two distinct regions. The first region is characterized by a linear dynamic range usually extending from the lower limit

of detection up to about 10^{-5} M, within which the signal response increases linearly with increasing concentration. In a second region encompassing progressively higher concentrations, the signal intensity levels off and finally decreases as concentration is further raised [2]. However, the rate of increase in the linear range, and the concentration at which the transition into the plateau region occurs, are variable. In this research, the linear dynamic range can be considered from 10^{-5} - 10^{-4} M for sulfur compounds. A possible interpretation of the effect of concentration on signal intensity was reported by Chowdhury et al. [30] and Smith et al. [31]. At elevated concentrations, the competition between analyte and electrolyte for the limited number of surface area available for charge localization on the droplets is increased. Therefore, the relative abundance of charged analyte ions is consequently decreased. In other words, a “saturation” limit does exist, which could be responsible for the decrease in abundance of charged analyte ions at enhanced concentration. Therefore, the presence of high quantities of added electrolytes will result in the suppression of analyte signals [34].

3.6 Effect of Concentration Ratio between Organosulfur Compounds and PdCl₂

The effect of the concentration ratio between sulfur compounds and PdCl₂ on the intensity and S/N ratio was studied by performing MS full scan for 1mM DBT with PdCl₂ at different concentrations. At the beginning stage of this research, formation of complex between sulfur and palladium was considered as the mechanism for enhancing molecular ion signals of sulfur compounds. So an excess amount of PdCl₂ (S: PdCl₂= 1:5) was applied. The results described in section 3.2 suggest that formation of radical cation might be caused by charge transfer from palladium complex to the sulfur compound.

Therefore, the ratio study can be a method to confirm this assumption. The results in Table. 3.4 demonstrate that stoichiometric amounts are not necessary to obtain a stable molecular ion signal for the sulfur compounds. On the contrary, with a decrease of PdCl₂ concentration, the signal intensity of the molecular ion peak increases and so does the S/N ratio. One explanation for this result is that complexation is necessary for charge transfer, but at concentrations above 10⁻⁵ mM, increasing the concentration of Pd doesn't enhance the signal intensity. Assuming charged Pd ions are distributed on the surface of a droplet in the spray region, the capacity of the droplet will be saturated at a certain concentration level. Only organosulfur compound near to the surface can undergo a complexation reaction with the Pd. Excess organosulfur compounds in the interior of the drop would not react. Therefore decreasing concentration of Pd doesn't decrease the molecular cation formation. In a future study, the concentration will be lowered to 10⁻⁵ mM. The samples were mixed in a tee instead of premixing in this study.

Ratio of DBT: PdCl ₂	Signal Intensity (10 ⁵)			Ratio of Signal Intensity between DBT and PdCl ₂	
	DBT	PdCl ₂ (147)	PdCl ₂ (248)	DBT: PdCl ₂ (147)	DBT: PdCl ₂ (248)
1:5	3.01	6.74	2.89	0.46	1.06
1:1	3.51	4.04	2.24	0.87	1.57
1:0.5	4.57	2.80	1.50	1.64	3.05
1:0.25	15.30	3.74	1.84	4.09	8.33
1:0.1	18.04	2.61	1.61	6.91	11.21

Table. 3.4 Study of ratio between DBT and PdCl₂. MS, full scan, 1mM DBT was dissolved in (50:50) CH₃OH: CH₃CN, source fragmentation voltage, 15v. T-tube injection system was used.

3.7 ESI/MS of Standard Compounds Mixture in Tufflo

Fig. 3.6 is the MS full scan spectrum of the mixture of the five standard compounds in Tufflo. Tufflo is a hydrogenated hydrocarbon matrix.

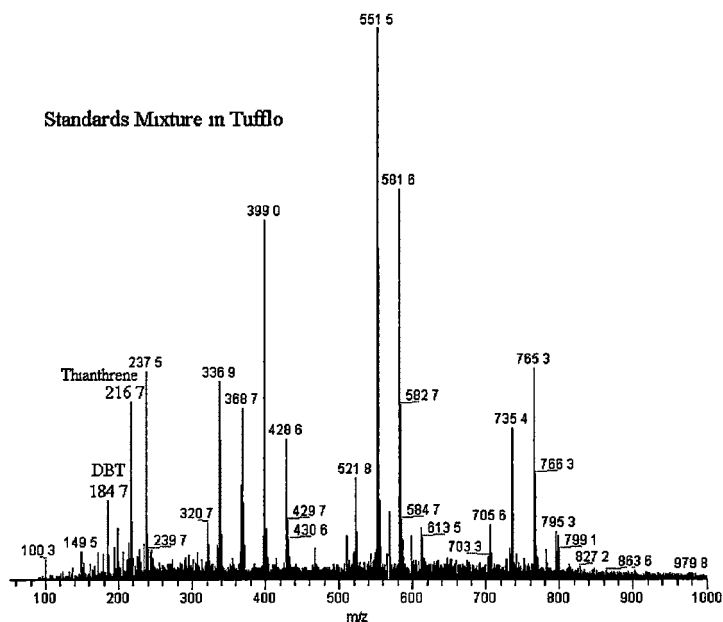


Fig. 3.9 MS full scan of standard mixture in Tufflo. 0.01g standard mixture and Tufflo with 0.025mM PdCl₂ in (50:50) methanol: acetonitrile; source fragmentation voltage, 15v.

Because of the strong and noisy response of Tufflo, only DBT and thianthrene showed signals in the full scan spectrum. However, BNTP, 2-DBT and 4,6-DBT had responses above 10⁵. The results suggest the MS characterization method is selective and applicable to organosulfur compounds even in a complicated chemical environment.

3.8 ESI/MS/MS of Organo Sulfur Compounds

3.8.1 Full Scan Mode

Fig. 3.10 shows the ESI/MS/MS full scan of DBT, thianthrene, BNTP, 2-DBT and 4,6-DBT.

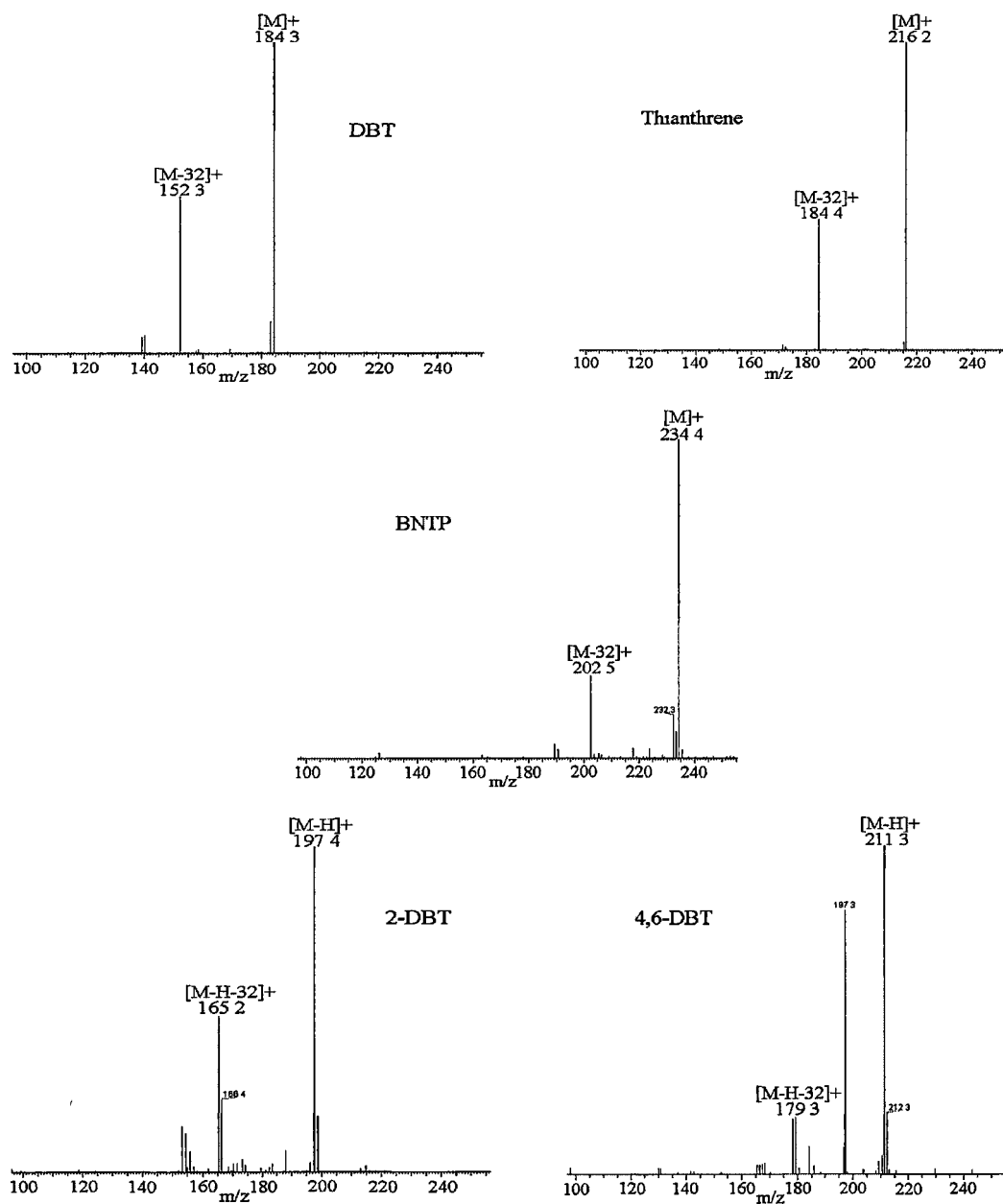


Fig.3.10 MS/MS full scan data for standards mixture. 1mM DBT, thianthrene, BNTP, 2-DBT and 4,6-DBT in 2mM PdCl₂, in (50:50) CH₃OH: CH₃CN.

The first three compounds have parent ions which are stable radical cations, while the other two compounds have parent ions missing one hydrogen. All of these five sulfur compounds have a consistent 32 neutral loss, which is believed to be a sulfur ion. The signal intensities of product ions losing a sulfur were all above 10^5 . To confirm that the 32 neutral loss is a sulfur, a MS^3 experiment was performed on thianthrene, which has two sulfur ions in its structure. In the MS^3 experiment, the product ion of MS^2 is fragmented by collision-induced-dissociation (CID). For thianthrene another 32 loss from the product ion of MS/MS was expected. The result demonstrated in Fig. 3.11 confirms these assumptions.

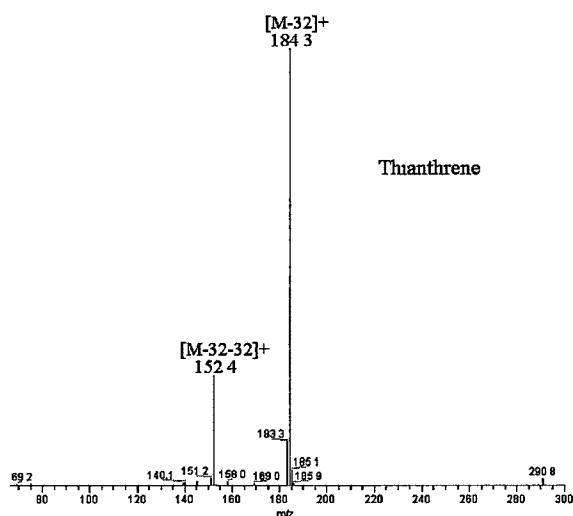


Fig. 3.11 ESI/ MS^3 full scan of thianthrene. 1mM with 5mM $PdCl_2$ in (50:50) CH_3OH :
 CH_3CN ; source fragmentation energy 25V, normalized collision energy at m/z 216 and
184 were 30% and 35% respectively.

Unlike the other species in the mixture, 2-DBT and 4,6-DBT showed parent ions missing a hydrogen. It is suspected that the methyl groups on these two compounds lose one hydrogen during the ionization and CID process [32]. Fig 3.12 illustrates the process.

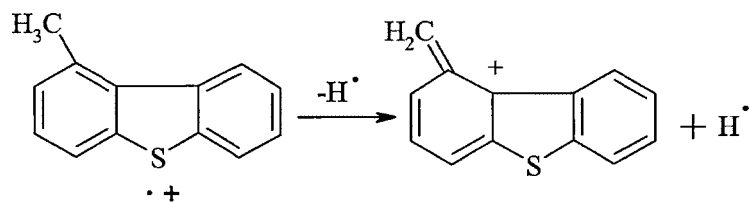


Fig. 3.12 The mechanism of hydrogen loss.

In radical cations, the charge is delocalized over the whole molecule. The most favored radical and charge sites in the molecular ion are assumed to arise from the loss of the electron of lowest ionization energy in the molecule. As the following order $n^- > \pi^- > \delta^-$ electrons is observed for ionization, the heteroatoms with weak ionization energies carry the charge preferentially [1]. For radical cations of organosulfur compounds theory suggests that the sulfur is the atom carrying the charge and radical.

Positive charge and radical sites are electron-deficient sites and can initiate cleavage reactions. The two kinds of cleavage reactions are called “charge-site-initiated reaction” (β cleavage) and “radical-site-initiated fragmentation” (α cleavage), respectively (Fig.3.13).

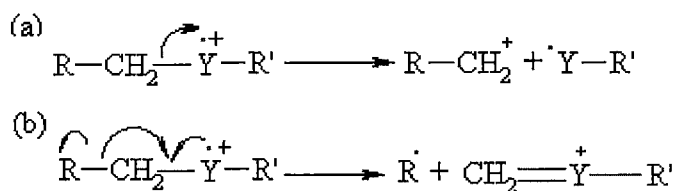


Fig. 3.13 Cleavage reactions of radical cation. (a) charge-site-initiated reaction; (b) radical-site-initiated fragmentation.

A cleavage reaction initiated by the positive charge site involves the attraction of an electron pair. The transfer of an electron pair induces heterolytic cleavage with the migration of the charge site. A cleavage reaction initiated by a radical site arises from the

strong tendency for a radical to form an electron pair. In this case, an odd electron is donated to form a new bond while concurrently the transfer of a second electron induces homolytic cleavage with migration of the site of the unpaired electron.

Based on the MS/MS spectrum of these compounds the mechanism of fragmentation is considered to be a charge-site-initiated reaction followed by a radical-site-initiated fragmentation. Taking the example of DBT, Fig. 3.14 shows a possible mechanism. First, the bond adjacent to the sulfur is broken by attraction of an electron pair from this bond. This cleavage can be seen as a direct dissociation assisted by inductive electron withdrawal due to the difference in electronegativity, but it occurs after the initial ionization to the radical cation. Finally odd electron migration initiates a bond cleavage to release the sulfur.

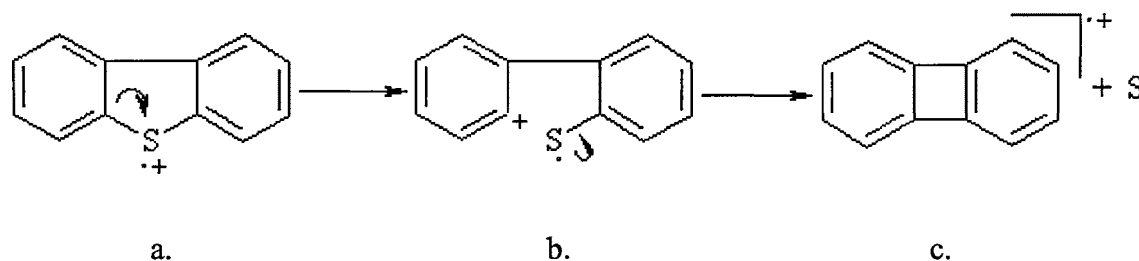


Fig. 3.14 Fragmentation mechanism of DBT.

The fragmentation processes for 2-DBT and 4,6-DBT are different from the other three. Besides losing one hydrogen, they also lose a 33 (HS) and 15 (CH_3) neutral fragment from the original molecular ion. The possible fragmentation mechanisms are proposed below in Fig. 3.15 [1,30].

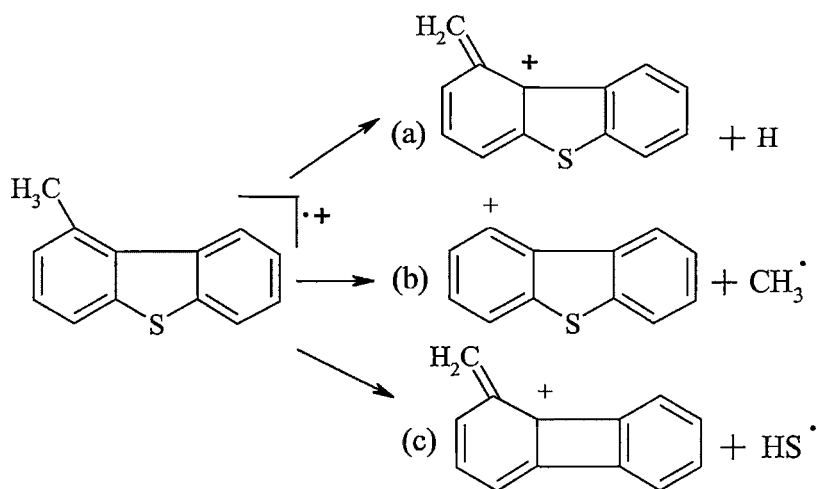


Fig. 3.15 Fragmentation mechanism of 2-DBT.

3.8.2 MS/MS SIM Mode

Single ion monitoring (SIM) is a technique in which particular ion or set of ions is monitored. Because only a few ions are monitored, SIM can provide lower detection limits and greater speed than a full scan.

As shown in Fig. 3 16, even at a concentration of 10^{-5}M , the molecular ions as well as the product ions with a 32 loss can be detected, and the signal intensities are still above 10^4 . The noisy background is due to the low concentration of sulfur compounds in these experiments. The results suggest that the SIM mode is useful in obtaining a low limit of detection.

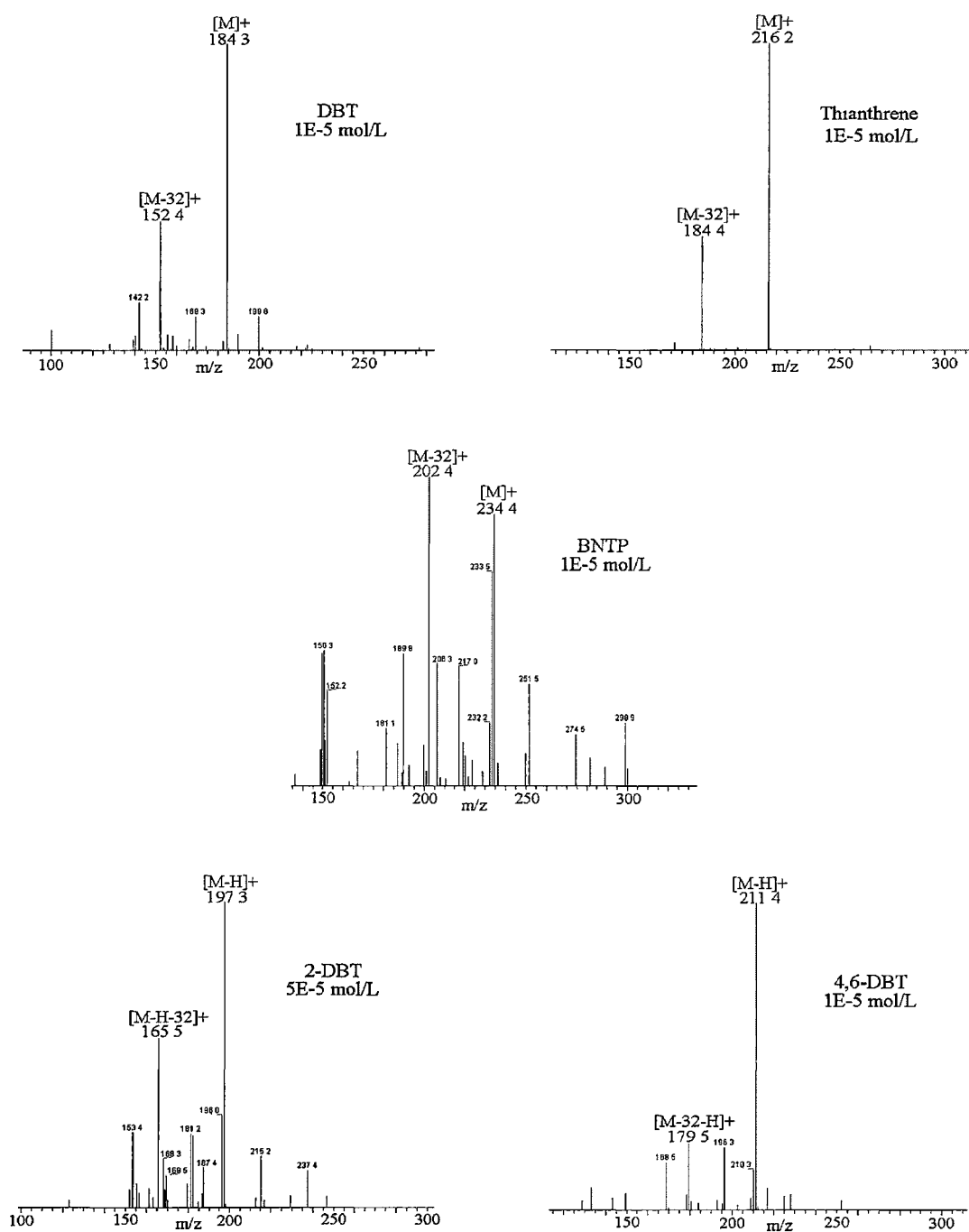


Fig. 3.16 MS/MS SIM data for standards mixture of DBT, Thianthrene, BNTP, 2-DBT and 4,6-DBT, 1mM with 2mM PdCl₂, in (50:50) CH₃OH: CH₃CN; source fragmentation energy, 15v. Normalized collision energies were 44%, 32%, 48%, 41% and 42% respectively.

3.9 Effect of Collision Energy

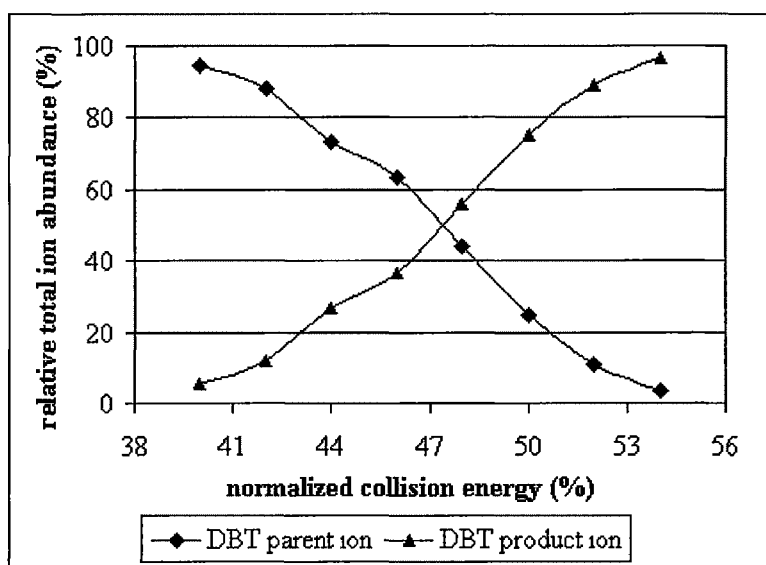
Fig. 3.17 shows the effect of increasing the collision energy on the fragmentation of DBT and BNTP. Collision energy of about 30% is the minimum required in order to observe a stable $[M-32]^+$ peak. The fragmentation pattern of losing a sulfur is stable for both DBT and BNTP. The relative signal intensity of product increases with increasing collision energy while the signal of the parent ion decreases. The relative signal intensity was calculated by taking the absolute intensity divided by the total ion signal intensity (product + parent).

The CID in an ion trap is defined as a low-energy collision (1-100eV). The kinetic energy arising from collision with inert gas is converted into internal energy, which causes molecular dissociation [1]. As observed in the results, the kinetic energy needs to meet a certain level (appearance potential) to transfer enough energy to a molecule in order to induce dissociation.

Fig. 3.18 shows the effect of increasing collision energy on 2-DBT and 4,6-DBT, which have more complicated fragmentation patterns than DBT and BNTP. These two compounds fragment into three different product ions. Initially the $[M-H]$ fragmentation mechanism is prominent but as the collision energy increases the loss of CH_3 and S begin to assume increasing importance. Sulfur appears to be the most difficult species to remove in alkyl substituted organosulfur compounds. The competition of three fragmentation mechanisms causes the decrease in the $[M-H]$ signal intensity at increasing collision energy. This phenomenon was observed before by Airiau et al [8]. Increasing the collision energy decreases the intensity of high mass fragment ions, while low range fragment ions increase in intensity. Moreover, in some cases, increasing the collision

energy further does not lead to further useful structural information: the signal becomes broader and dominated by noise.

(a)



(b)

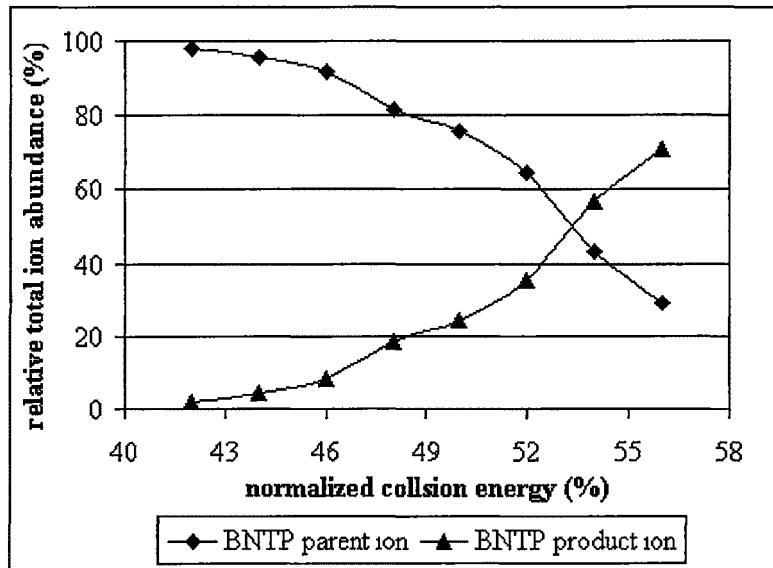
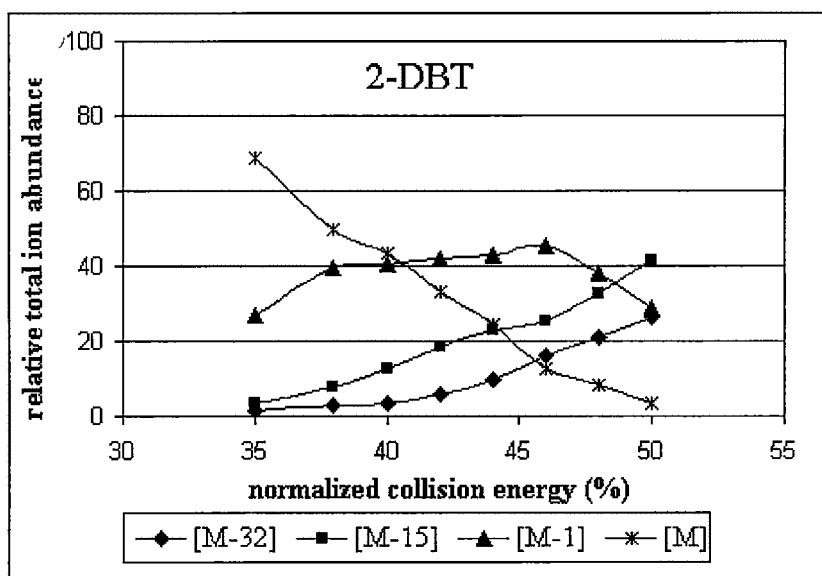


Fig. 3.17 Effect of ion trap collision energy on fragmentation of DBT and BNTP. Source fragmentation energy was 15V.

(a)



(b)

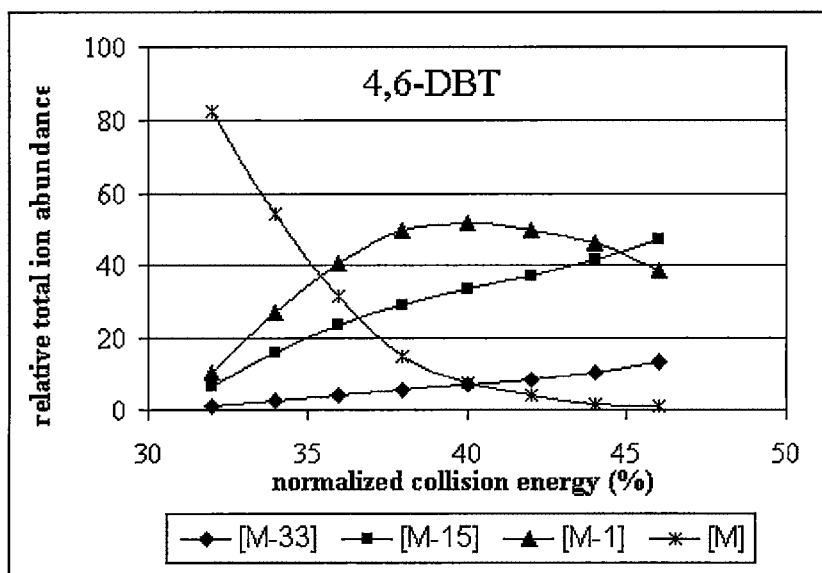


Fig. 3.18 Effect of ion trap collision energy on fragmentation of 2-DBT and 4,6-DBT. Source fragmentation energy was 15V.

3.10 ESI/MS and MS/MS of Maya Crude Oil Fractions

ESI/MS and MS² experiment were performed for the CMSPAC and CMPASH fractions from a Maya crude oil. The results of MS are shown in Fig. 3.19.

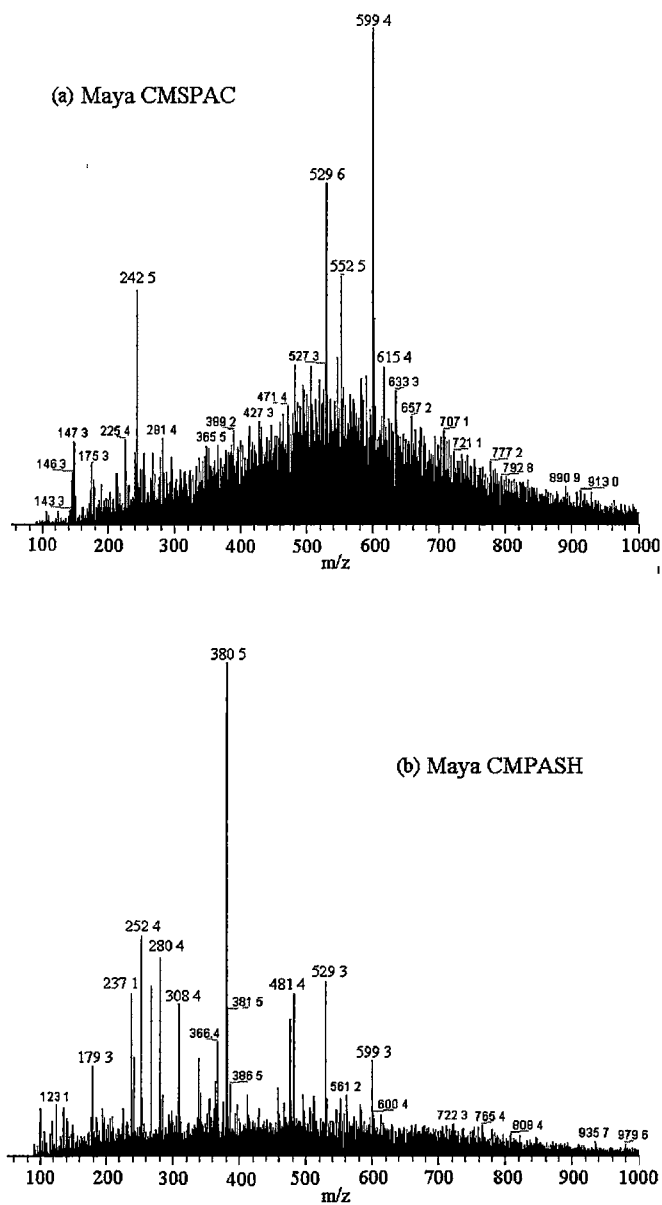


Fig. 3.19 MS full scan of Maya crude oil, fraction (a) CMSPAC and (b) CMPASH. 1mg in 1ml (50:50) CH₃OH: CH₃CN. Source fragmentation voltage, 15V

Unlike the sample preparation used for the standard compounds, both of the two fractions contained PdCl_2 which was introduced during the course of the separation on the $\text{PdCl}_2/\text{silica}$ column. As the spectra suggest, the mass distribution of CMSPAC is centered around 529 and that of CMPASH around 480.

Some major peaks with high abundance were picked to perform MS/MS for each fraction. The results are shown in Fig. 3.20.

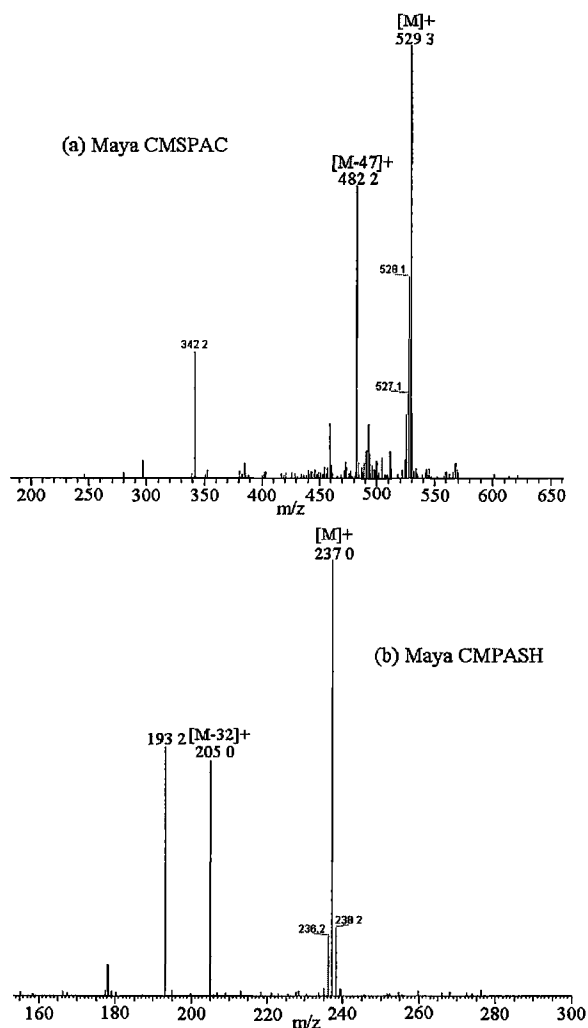


Fig. 3.20 MS/MS full scan data for Maya crude oil, (a) a peak from fraction CMSPAC; source fragmentation energy, 10v and (b) a peak from fraction CMPASH; source fragmentation energy 15v.

For CMSPAC, peaks at m/z 599, 529, 552, 615 were fragmented in the ion trap to obtain further structural information. A constant neutral loss of 47 was observed consistently for every peak, which is believed to be a CH_3S fragment [1,32]. The fragmentation pattern for the peak at 529 is shown in the spectrum represented in Fig. 3.20a.

For CMPASH, peaks with m/z 237, 252, 280 were explored using MS/MS experiments. Peak 252 and 280 showed a loss of 57. Neutral loss 32 (S), 33 (HS) or 47 (CH_3S) are generally considered an indication of the presence of sulfur. Therefore a loss of 57 does not suggest sulfur. A neutral loss of 57 can be a butyl group (C_4H_9). The even numbers for the molecular ion exclude the possibility that they have an odd number of nitrogens in their structure. Furthermore, the 28 mass difference of these two peaks, which have similar fragmentation patterns shows the only structural difference between them may be two methylene groups. However, except for sulfur, it is not clear if the two compounds have any other heteroatoms in their structures, such as oxygen or an even number of nitrogens. Peak 237 had a 32 and 44 neutral loss. From our work, a loss of 32 suggests a sulfur, while from our previous work in naphthenic acids, a loss of 44 suggests a COOH group. Furthermore, this peak has an odd m/z , which suggests the presence of a nitrogen atom. Based on results obtained before, only organosulfur compounds having 3 or more rings provide an observable response in MS. Therefore this molecule is probably a structure with three or more rings, containing a sulfur atom, a nitrogen atom and a carboxyl group. The spectrum in Fig. 3.20b shows the results of MS/MS on peak 237. The possible formula is $\text{C}_{12}\text{H}_{15}\text{NSO}_2$ and a possible structure is proposed in Fig.3.21.

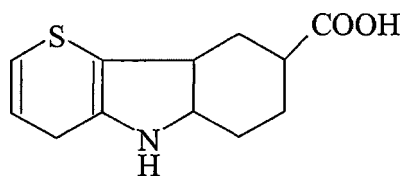


Fig. 3.21 The possible structure of the compound with M.W. 237 in CMPASH.

These results show the power of MS/MS to provide structural information on unknown compounds in crude oil.

CHAPTER IV

CONCLUSION

ESI/MS and ESI/MS/MS were performed on organosulfur standard compounds and CMSPAC and CMPASH fractions isolated from a Maya crude oil. Source fragmentation energy, concentration, collision energy and the concentration ratio between sulfur compounds and PdCl₂ have effects on the formation of molecular ions or compound fragmentations. The presence of PdCl₂ in the sample solution enhances the formation of molecular ions due to complexation followed by a charge transfer reaction between the sulfur compounds and palladium. For nonalkylated species, radical cations of sulfur compounds are formed in the ESI source. Alkylated species exhibit the loss of H and the alkyl group. In MS/MS experiments, a neutral loss of 32 (S) is consistent for most of the standard sulfur compounds and 33 (HS) for alkylated species. Therefore, compounds containing organic sulfur can be identified by performing tandem MS under the proper conditions.

REFERENCES

1. Hoffmann, E.; Stroobant, V. *Mass spectrometry, Principles and Applications* **1999**, Wiley, Chichester.
2. Cole, R. B. *Electrospray Ionization Mass Spectrometry* **1997**, Wiley, Chichester.
3. Fenn, J. B.; Mann, M.; Meng, C. K.; et al *Science* **1989**, 246, 64-71.
4. Snyder, A. P. *Biochemical and Biotechnological Applications of Electrospray Ionization Mass Spectrometry* ACS Symposium Series 619, American Chemical Society, Washington, DC, **1996**.
5. Mora, J. F.; Van Berkel, G. J.; Enke, C. G., et al *J Mass Spectrom.* **2000**, 35, 939.
6. McLafferty, F. W.; *Tandem Mass Spectrometry* **1983** , New York.
7. Busch, K. L.; Glish, G. L.; McLuckey, S.A. *Mass Spectrometry/Mass Spectrometry: Techniques and Applications of Tandem Mass Spectrometry* **1988**, VCH, New York.
8. Airiau, C. Y.; Brereton, R. G.; Crosby, J. *Rapid Communications in Mass Spectrometry* **2001**, 15, 135-140.
9. Speight, J. G. *Fuel Science and Technology Handbook*; Marcel Dekker: New York, 1990.
10. Whitehurst, D.; Isoda, T.; Mochida, I. *Adv Catal* **1998**, 42, 345-471.
11. Martin, R. L.; Grant, J. A. *Anal. Chem.* **1965**, 37, 644-649.

27. Christensen, R. G.; White, E., *J. Chromatogr.* **1985**, 323, 33-36.
28. Bayer, E.; Gfroerer, P.; Rental, C.; *Angew. Chem. Int. Ed.* **1998**, 38, 992-995.
29. Hartley, F. R. *The Chemistry of Platinum and Palladium* **1973**, John Wiley & Sons, Inc, New York.
30. Chowdhury, S. K.; Katta, V.; Chait, B. T. *Rapid Commun. Mass Spectrom.* **1990**, 4, 81-87.
31. Smith, R. D.; Loo, J. A.; Edmonds, C. G.; Barnaga, C. J.; Udseth, H. R. *Anal. Chem.* **1990**, 62, 882-899.
32. Silverstein, R. M.; Webster, F. X. *Spectrometric Identification of Organic Compounds* **1998**, John Wiley & Sons, Inc, New York.
33. Lias, S. G.; Bartmess, J. E.; Liebman, J. F.; Holmes, J. L.; Levein, R. D.; Mallard, W. G. *J Phys. Chem. Ref Data* **1998**, 17 (Suppl. 1).
34. Tang, L.; Kebarle, P. *Anal. Chem.* **1993**, 65, 3654-3668.
35. Tang, L.; Kebarle, P. *Anal. Chem.* **1991**, 63, 2709-2715.